REPUBLIC OF TURKEY
BİNGÖL UNIVERSITY
INSTITUTE OF SCIENCE

DECIPHERING THE ROLE OF KNOCKDOWN TIGAR IN THE LUNG CANCER CELL LINE THROUGH REGULATION PROGRAMED CELL DEATH

DOCTORAL THESIS

Osama Hamid SHAREEF

BIOLOGY DEPARTMENT

SUPERVISOUR:
Assistant Prof. Dr. Can Ali AĞCA

BİNGÖL-2019

REPUBLIC OF TURKEY
BİNGÖL UNIVERSITY
INSTITUTE OF SCIENCE

DECIPHERING THE ROLE OF KNOCKDOWN TIGAR IN THE LUNG CANCER CELL LINE THROUGH REGULATION PROGRAMED CELL DEATH

This dissertation, created by Osama Hamid SHAREEF under supervision of Asst. Prof. Dr. Can Ali AĞCA, was accepted as a PhD thesis in department/discipline of BIOLOGY / MOLECULAR BIOLOGY AND GENETICS by the following committee on 15/01/2019 with the vote unity.

Head of examining committee:	Prof. Dr. Mehmet ÇİFTCİ	*Signature* :
Member	: Assoc. Prof. Dr.Abdullah ASLAN	*Signature*:
Member	: Asst. Prof. Dr. Can Ali AĞCA	*Signature* :
Member	: Asst. Prof. Dr. Sabahattin CÖMERTPAY	*Signature* :
Member	: Asst. Prof. Dr.M. Kadir ERDOĞAN	*Signature* :

This result has been approved on ...../..../2019 with the decision of ……/…… by Board of Directors of the Science Institute.

Assoc. Prof. Dr. Zafer ŞİAR
Director of the institute

This study was supported within the scope of Bingöl Üniversitesi Bilimsel Araştırma Proje (BÜBAP).
Project No: BAP-FEF.2016.00.012

Not: Bu tezde kullanılan özgün ve başka kaynaklardan yapılan bildirişlerin, çizelge, şekil ve fotoğrafların kaynak olarak kullanımı, 5846 sayılı Fikir ve Sanat Eserleri Kanunundaki hükümLere tabidir.

ACKNOWLEDGMENT

I must thank "ALLAH" for giving me the opportunity and ability to finish my PhD.

Deepest gratitude for the enthusiastic supervision of dear Asst. Prof. Dr. Can Ali AĞCA, who was abundantly helpful and offered invaluable assistance without counting times. Honestly, his advices and his knowledge encouraged me to effort in this project; I have got huge information for the project time, and hope a brilliant future for him and see him in the one of the worldwide scientists.

Special thanks also to Prof. Dr. Victor NEDVZVETSKI, who contributed his time within the lab, he helped me to understand and I appreciate the techniques used.

I would like to express special gratitude and thanks to Asst. Prof. Dr.Mehmet Kadir ERDOĞAN, Asst. Prof. Ekrem DARENDELİOĞLU, Asst. Prof. Dr. Musa TARTIK and research assistant Gürkan AYKUTOĞLU they contributed their times with me every time.

My deepest gratitude goes to my long suffering wife (Hero), whose support made this whole adventure possible. I must thank "ALLAH" for granting me by lovely blessing kids (Maily and Ahmad) during the course of my study; by whom I was always inspired.

I would like to forward my deepest thanks for my dear respect parents and my family members, which they were with me. My thankfulness for my friends and classmates and those who in any way were helpful in making my research ready.

I would like to mention BUBAP office (Project Number: BAP-FEF.2016.00.012) in Bingol University for supporting financially my thesis.

Osama Hamid SHAREEF

Bingöl 2019

TABLE OF CONTENTS

ACKNOWLEDGMENT…….. ii
TABLE OF CONTENTS..... iii
TERMS AND ABBREVIATIONS..... vi
LIST OF FIGURES…….. xi
LIST OF TABLES…… xii
ÖZET…… xiii
ABSTRACT…….. xiv

1. INTRODUCTION……. 1
1.1. Lung…… 1
1.2. Cancer……..... 2
1.2.1. Lung Cancer……. 3
1.2.2. Types of Lung Cancer…….. 4
1.2.2.1. Small Cell Lung Cancer…… 4
1.2.2.2. Non-Small Cell Lung Cancer…… 5
1.2.3. Classification Pathological Staging and Grading in Lung Cancer…… 5
1.3. Programmed Cell Death…….. 6
1.3.1. Apoptosis……... 6
1.3.1.1. Apoptosis and Cancer……. 7
1.3.1.2. Apoptosis Pathway…….. 8
1.3.1.2.1. Extrinsic Pathway……. 8
1.3.1.2.2. Intrinsic Pathway…….. 9
1.3.2. Autophagy…….. 11
1.3.2.1. Basic Autophagy Machinery…… 12
1.3.2.2. Autophagy and Cancer…… 14
1.3.2.2.1. Autophagy as Tumor Suppressor……. 15
1.3.2.2.2. Autophagy as Tumor Promoter……... 16

1.3.2.3. Autophagy as a Program Cell Death……. 17
1.3.3. Crosstalk between Apoptosis and Autophagy…….. 18
1.4. TP53-Induced Glycolysis and Apoptosis Regulator…… 19
1.5. Oxidative Stress and Cancer…… 20
1.5.1. NADPH Oxidase……... 20
1.5.2. Reactive Oxygen Species……. 20
1.5.3. NFκB Pathway……. 21
1.5.4. HO-1 Pathway…….. 23
1.5.5. Oxidative Stress and Apoptosis…… 24
1.5.6. Oxidative Stress and Autophagy……... 25
1.5.7. The Antioxidant Activities of TIGAR…….. 25
1.6. Aims and Objectives…… 25

2. MATERIALS AND METHODS…… 26
2.1. General……. 26
2.2. Thawing and Recovering Cell…….. 32
2.3. Cell Splitting and Maintenance…… 33
2.4. Transfection with Small Interfering RNAs (siRNA)…… 33
2.5. Measurement of Cell Viability……. 34
2.6. Clonogenic Survival Assay…….. 34
2.7. Total Cellular ROS Levels…… 34
2.8. Measurement of NADPH Levels……. 35
2.9. Protein Extraction and Western Blot Analysis……. 35
2.9.1. Cell Lysate……. 35
2.9.2. Bradford Protein Assay……. 36
2.9.3. Sample Preparation for Loading…… 36
2.9.4. SDS-PAGE…… 37
2.9.5. Immunoblotting (Western Blot)……. 38
2.9.6. Blotting Procedure……. 38
2.9.7. Blocking the Membrane……. 39
2.9.8. Membrane Labeling…… 40
2.9.9. Detection……. 41
2.10. RNA Extraction and qRT-PCR…… 41

2.10.1. Total RNA Isolation…….. 41
2.10.2. cDNA Synthesis…….. 42
2.10.3. Real Time PCR…… 42
2.11. Statistical Analysis…….. 43

3. RESULTS…… 44
3.1. siRNA and BPA…… 44
3.2. TIGAR-siRNA Down-Regulates TIGAR Expression in A549 Cells…….. 45
3.4. TIGAR Knockdown Induces an Decreasing NADPH Level via ROS…… 48
3.5. TIGAR-Specific siRNA up-Regulates Apoptosis Markers…… 49
3.6. TIGAR-Specific siRNA up-Regulates Autophagy Markers……. 51
3.7. TIGAR-Specific siRNA up-Regulates Oxidative Stress Markers…….. 52

4. DISCUSSION…… 54

5. CONCLUSION…….. 59

REFERENCES…….. 60

CURRICULUM VITAE…… 73

TERMS AND ABBREVIATIONS

AGO	: Argonaute
AIF	: Apoptosis-Inducing Factor
AMPK	: Adenosine Monophosphate-Activated Protein Kinase
AP1	: Activator protein 1
APAF-1	: Apoptotic Protease Activating Factor 1
ARE	: Antioxidant Response Element
ATG-6 (Beclin-1)	: Autophagy Related Gene 6
ATP	: Adenosine Triphosphate
BAK	: Bcl-2 Homologous Antagonist Killer
BAX	: Bcl-2-Associated X
Bcl-2	: B-Cell Lymphoma 2
BH3	: Bcl-2 Homology Domain 3
BID	: BH3 Interacting Domain Death
BIF-1	: Baxinteracting Factor-1
BSA	: Bovine Serum Albumin
BUCR	: Bingol University Cancer Research Centre
Caspase-3	: Cysteine-Aspartic Proteases-3
CD163	: Cluster of Designation
cDNA	: Complementary DNA
CMA	: Chaperone Mediated Autophagy
CMA	: Chaperone-Mediated Autophagy
CO_2	: Carbon Dioxide
COPD	: Chronic Obstructive Pulmonary Disease
CREB	: cAMP Response Element Binding
DAPK	: Death-Associated Protein Kinase
DCFDA	: Dichlorodihydrofluorescein Diacetate

ddH_2O	: Double-Distilled Water
DMSO	: Dimethyl Sulfoxide
DNA	: Deoxyribonucleic Acid
dsRNA	: Double-Stranded RNA
ECL	: Enhanced Chemiluminescence
ECM	: Extracellular Matrix
EDTA	: Ethylen Ediamine Tetra Acetic Acid
EGTA	: Ethylene Glycol Tetra Acetic Acid
ELISA	: Enzyme Linked Immunosorbent Assay
ER	: Endoplasmic Reticulum
ER	: Endoplasmic Reticulum
Ex / Em	: Excitatio and emission
FADD	: Fas-Associated Protein with Death Domain
FAS	: First Apoptosis Signal Receptor
FBS	: Fetal Bovine Serum
Fru-2, 6-P2	: Fructose-2,6- Bisphosphate
G6PD	: Glucose-6-Phosphate Dehydrogenase
GAPDH	: Glyceraldehyde 3-Phosphate Dehydrogenase
gDNA	: Genomic Deoxyribonucleic Acid
GSH	: Glutathione
GTPase	: Guanosine Triphosphate
H	: Hour
H_2O_2	: Hydrogen Peroxide
HCC	: Hepatocellular Carcinoma
HIF-1α	: Hypoxia-Inducible Factor 1-Alpha
HO-1 or HMOX1	: Heme Oxygenase 1
I/R	: Ischemia/Reperfusion
IBD	: Inflammatory Bowel Disease
IFN	: Interferon Gamma
IKKα	: Inhibitory Kappa B Kinase α
IL-1	: Interleukin (IL)-1
IRS-1	: Insulin Receptor Substrate 1
JNK-1	: Jun N-Terminal Kinase

Kda	: Kilo Dalton
LAMP-2A	: Lysosomal-Associated Membrane Protein 2A
LAMP-2A	: Lysosomal-Associated Membrane Protein 2A
LC3	: Light Chains-3
LKB-1	: Liver Kinase B1
LPS	: Lipopolysaccharide
mA	: Milliampere
MCL-1	: Myeloid Cell Leukemia 1
Min	: Minute
mL	: Milliliter
mM	: Millimolar
MOMP	: Mitochondrial Outer Membrane Permeabilization
mRNA	: Messenger Ribonucleic Acid
mTOR	: Mammalian Target of Rapamycin
NADPH	: Nicotinamide Adenine Dinucleotide Phosphate
NF-κB or RelB	: Nuclear Factor Kappa-Light-Chain-Enhancer of Activated B Cells
NIK	: NF-Kappa-B-Inducing Kinase
NO	: Nitric Oxide
NOS	: Nitric Oxide Synthase
NOX	: NADPH Oxidases
NRF2	: Nuclear Factor Erythroid 2–Related Factor 2
NSCLC	: Non-Small Cell Lung Cancer
ODS	: Optical Densities
PBS	: Phosphate Buffered Saline
PCD	: Programmed Cell Death
PDGF	: Platelet Derived Growth Factor
PFK-2/FBPase-2	: Phosphofructokinase-2 or Fructose Bisphosphatase-2
PH	: Potential Hydrogen
PI3K	: Phosphoinositide 3-Kinase
PKB (AKT)	: Protein Kinase B
PMSF	: Phenylmethane Sulfonyl Fluoride
PPP	: Pentose Phosphate Pathway
PTEN	: Phosphatase and Tensin Homolog

PVDF	: Poly-Vinylidene Fluoride
qRT PCR	: Quantitative Real Time Polymerase Chain Reaction
REDD1	: Regulated In Development And Dna Damage Response 1
RHEB	: Ras Homolog Enriched in Brain
RISC	: RNA-Induced Silencing Complex
ROS	: Reactive Oxygen Species
RPM	: Revolutions Per Minute
RPMI	: Roswell Park Memorial Institute
RVFV	: Rift Valley Fever Virus
SCLC	: Small Cell Lung Cancer
SDS	: Sodium Dodecyl Sulfate
SDS-PAGE	: Sodium Dodecyl Sulfate Polyacrylamide Gel Electrophoresis
shRNA	: Short Hairpin RNA
siRNA	: small (or short) interfering RNA
SMAC	: Second Mitochondria-Derived Activator of Caspase
SOD	: Superoxide Dismutase
STK-11 (LKB-1)	: Serine/Threonine Kinase 11
TBA	: Thiobarbituric Acid
TBI	: Traumatic Brain Injury
TBS	: Tris-Buffered Saline
TBST	: Tris Buffered Saline Tween
TCA	: Trichloroacetic Acid
TEMED	: Tetramethylethylenediamine
TIGAR	: Tp53-Induced Glycolysis and Apoptosis Regulator
TLR4	: Toll-Like Receptors
TNF	: Tumor Necrosis Factor
TRAIL	: TNF-Related Apoptosis-Inducing Ligand
TSC 1, 2	: Tuberous Sclerosis
TXNL2	: Thioredoxin-Like 2
ULK 1, 2	: Unc-51 Like Autophagy Activating Kinase
UVRAG	: Ultraviolet Radiation Resistance-Associated Gene
VEGF	: Vascular Endothelial Growth Factor
VHL	: Von Hippel-Lindau

VPS34	: Vacuolar Protein Sorting 34
WST-1	: Water Soluble Tetrazolium -1
µg	: Microgram
µL	: Microliter
µM	: Micrometer
µmol	: Micromole

LIST OF FIGURES

Figure 1.1. It shows anatomy of the upper and lower parts of human……. 2
Figure 1.2. Schematic diagram shows the development…….. 3
Figure 1.3.Schematic representations of apoptotic events…….. 10
Figure 1.4. Molecular entities and mechanisms that regulate autophagy…… 14
Figure 1.5. NF-κB pathways…… 22
Figure 1.6. It shows the HO-1 pathways……. 24
Figure 2.1. Making western blotting by Bio-Rad System……... 39
Figure 3.1. It shows the A549 cells under microscope…… 44
Figure 3.2. Protein standard assay curve showing the absorbency……. 45
Figure 3.3. siRNA TIGAR knockdown in A549 cells…… 47
Figure 3.4. siRNA TIGAR knockdown inhibited cell viability…….. 48
Figure 3.5. siRNA TIGAR knockdown enhances an increasing ROS…… 49
Figure 3.6. siRNA TIGAR knockdown induced apoptosis of A549 cells……... 50
Figure 3.7. siRNA TIGAR knockdown enhances autophagy……. 52
Figure 3.8. siRNA TIGAR knockdown enhances oxidative stress markers…… 53

LIST OF TABLES

Table 2.1. All chemicals, reagents and materials…… 26
Table 2.2. All kits were used for the experiments……... 28
Table 2.3. All devices and equipment's were used in the experiments……... 28
Table 2.4. Solution names and their components…… 29
Table 2.5. Solutions were used for tris/glycine sds…….. 37
Table 2.6. The primary and secondary antibodies…….. 40
Table 2.7. The secondary antibodies were used in Immunoblotting assay……... 40
Table 2.8. The real-time cycler was set up…… 43
Table 2.9. It shows the sequences of primers…… 43

AKCIĞER KANSERI HÜCRE HATTINDA, KNOCKDOWN TIGAR'IN PROGRAMLI HÜCRE ÖLÜMÜNÜN DÜZENLENMESINDEKI ROLÜNÜN DEŞIFRE EDILMESI

ÖZET

Küçük hücreli olmayan akciğer kanseri ölümcül bir malignite ile yüksek mortalite oranına sahiptir. siRNA, gen ifadesinin negatif düzenleyicileri olarak transkripsiyon sonrası süreçte protein kodlayan genlerin kısa süreli susturulmasını indüklemek için en yaygın kullanılan RNA interferens aracıdır. TIGAR proteini,glikoz metabolizması sırasında Fru-2, 6-P2 seviyelerini kontrol eder ve NADPH düzeyini devam ettirerek hücre içi önemli birantioksidan olan GSH'nin geri dönüştürmesine yardımcı olur. TIGAR'ın işlevlerinden biri, hücrelerdeki Fru-2, 6-P2 seviyelerini düşürmek ve sonuç olarak hücre ölümüne karşı daha yüksek dirençle korele olan ROS'u baskılamak ve glikolizi azaltmaktır. Bununla birlikte, siRNA'nın hücre canlılığı, oksidatif stres ve programlanmış hücre ölümleri üzerindeki etkileri veya siRNA'nın akciğer kanseri hücrelerinde TIGAR ile nasıl etkileştiği hakkında pek az şey bilinmektedir. Bu çalışma, A549 hücre hattında TIGAR'ın susturulmasının altında yatan moleküler mekanizmaları araştırmak için tasarlanmıştır.siRNA-TIGAR'ın A549 akciğer kanseri hücreleri üzerindeki etkisini saptamak için hücre canlılığını, koloni oluşumunu, ROS ve NADPH'nin oksidatif stres seviyelerini ve hücre canlılığını ölçmek için sırasıyla hücre proliferasyonu, koloni oluşumu, ROS ve NADPH analizleri gerçekleştirdik. Ek olarak, protein ve mRNA ekspresyon seviyelerini ölçmek için sırasıyla western blot ve real-time PCR analizleri kullanıldı.A549 hücre hattında TIGAR inaktif edildikten sonra çeşitli parametreler analiz edildi ve TIGAR'ın down regülasyonunun canlılığı inhibe ettiği ve koloni oluşumunu azalttığı gösterildi. Ayrıca TIGAR inaktivasyonunun apoptozis ve otofajiyi tetiklediği görüldü. Artmış ROS seviyeleri ve azalmış NADPH seviyelerine bağlı olarak oksidatif stres belirteçlerinin indüksiyonu gözlemlendi. Özetle, siRNA TIGAR hücre canlılığını inhibe edip programlanmış hücre ölümlerini (I, II) arttırmıştır ve ROS seviyesini artırarak yüksek oksidatif stres markırlarını yüksek düzeylere çıkarmıştır. Bulgular, TIGAR'ı susturmanın hücre canlılığı inhibisyonunu indüklediğini, ROS seviyelerini artırdığını, NADPH düzeylerini azalttığını, otofaji, apoptosis ve oksidatif stres belirteçlerini indüklediğini gösterdi. Genel olarak, bu çalışma kanser tedavisinde terapötik bir hedef olarak kullanılmak üzere akciğer kanseri hücrelerinde programlanmış hücre ölümü I, II'yi arttırmak için TIGAR susturmanın muhtemel rolünün anlaşılmasını desteklemektedir.

Anahtar Kelimeler: Tigar, akciğer kanseri, apoptoz, otofaji, oksidatif stres markerleri.

DECIPHERING THE ROLE OF KNOCKDOWN TIGAR IN THE LUNG CANCER CELL LINE THROUGH REGULATION PROGRAMED CELL DEATH

ABSTRACT

Non-small cell lung cancer has a high mortality rate with a lethal malignancy. siRNA is the most-commonly used RNA interference tool for inducing short-term silencing of protein-coding genes in the post-transcriptional process as negative regulators of gene expression. The TIGAR protein controls Fru-2, 6-P2 levels during glucose metabolism and helps maintain NADPH levels to recycle GSH, a key intracellular antioxidant. One of TIGAR's functions is to lower Fru-2, 6-P2 levels in cells, consequently decreasing glycolysis and suppressing ROS, which correlate with higher resistance to cell death. However, little is known about the effects of siRNA on cell viability, oxidative stress, and programmed cell deaths, or about how siRNA interacts with TIGAR in lung cancer cells. The present study was designed to investigate the molecular mechanisms underlying TIGAR knockdown in the A549 cell line.

To detect the influence of siRNA-TIGAR on A549 lung cancer cells, we performed cell proliferation, colony formation, ROS, and NADPH assays to measure cell viability, ability of cells to form colonies, and oxidative stress levels of ROS and NADPH, respectively. In addition, western blotting and real-time PCR assays were used to measure protein and mRNA expression levels, respectively.

After TIGAR-knockdown in A549 cell lines, various assay parameters were analyzed and showed that down regulation of TIGAR inhibited viability and decreased colony formation. We also demonstrated that TIGAR knockdown induced apoptosis and autophagy. Furthermore, increased ROS levels and decreased NADPH levels were observed, followed by an induction of oxidative stress marker expression. In summary, siRNA TIGAR inhibited cell viability, enhanced programmed cell deaths (I, II), and elevated oxidative stress markers by increasing ROS levels.

The data showed that TIGAR knockdown induced inhibition of cell viability; increased ROS levels; and decreased NADPH levels, induction of autophagy and apoptosis, and oxidative stress markers. Overall, this study supports our understanding the possibility of using TIGAR knockdown in lung cancer cells to enhance programmed cell death I, II for further use as a therapeutic target in cancer treatment.

Keywords: Tigar, lung cancer, apoptosis, autophagy, oxidative stress markers.

1. INTRODUCTION

1.1. Lung

Breathing in higher living organisms mainly involves lungs which serve as an important organ of the respiratory system. Besides lungs, mouth, nose, trachea (windpipe) and airways or tubes to both lungs are also parts of the respiratory system. As shown in Figure 1.1, the airways comprise of bronchioles (small airways) and bronchi (large airways). In appearance, the lungs look like two large, spongy cones. Sections in the lungs are termed as lobes. The right lung and left lung has three and two lobes. Diaphragm offer support to the lungs and is actually a thin and wide muscle which facilitates breathing. Mediastinum refers to the space between two lungs and carries structures like esophagus, lymph nodes, trachea, heart and blood vessels.

Two layers of pleura envelop the lungs. Pleura are tissue sheets with thickness of plastic wrap. Outer layer of pleura is known as parietal layer and it layers the diaphragm and chest wall. On the other hand, inner layer is termed as visceral layer which is linked to lungs. Pleural space between these two layers is called pleural cavity which carries a little quantity of fluid. Due to this fluid the two pleural layers slide over one another thereby allowing smooth movement of lungs against the wall of chest while breathing. Inhalation involves passage of air into mouth or nose to trachea and then into bronchi and bronchioles. Very small sized air sacs are present at the end of bronchioles which are termed as alveoli. These structures serve as site for the exchange of oxygen and carbon dioxide. Oxygen is delivered to blood and carbon dioxide is taken from the blood. Exhalation involves removal of carbon dioxide by breathing out (John 2005; Mothoneos 2016).

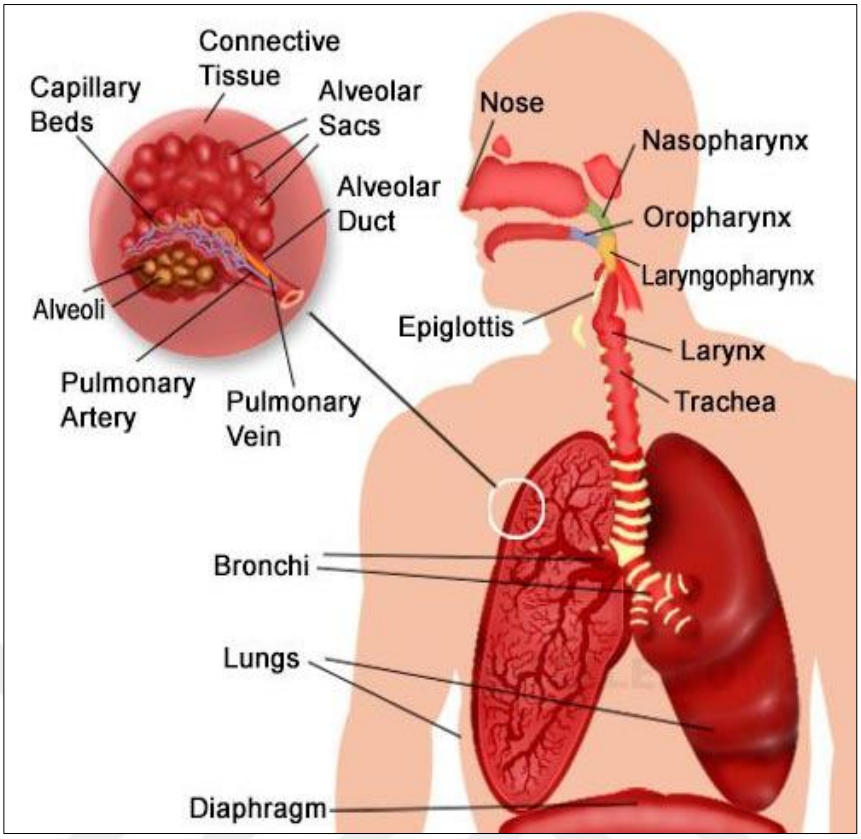

Figure 1.1. It shows anatomy of the upper and lower parts of human respiratory system(Kara Rogers Senior Editor 2010)

1.2. Cancer

‘‘Cancer cells are defined by two heritable properties: (1) reproduce in defiance of the normal restraints on cell division and (2) invade and colonize territories normally reserved for other cells. It is the combination of these actions that makes cancers peculiarly dangerous’’ (Alberts 2002). It may have an effect on almost any a part of the body. The growth regularly invades surrounding tissue and might metastasize to distant sites. New cells are produced in living systems for growth, healing and for replacing old cells. Production and death of cells generally takes place in an organized manner. Yet, in some cases, cells do not grow, divide and die as they are meant to be. Consequently, a lump is formed due to collection of abnormal blood or lymph fluid. This lump is termed as tumor. Tumors can be malignant or benign. Malignant tumors comprise of cancerous cells demonstrating the capability to spread to other areas via lymphatic system or bloodstream. On the other hand, benign tumors comprise of cells which remain confined to a specific area (Mothoneos 2016).

When cancer develops in an organ or tissue, it is termed as primary cancer. Malignant tumors are mostly named according to the cells or organ involved. Localized cancer refers to a malignant cancer which has not yet spread to other regions in the body. Surprisingly, a tumor can get deep into nearby tissues and can form its blood vessels by a process known as angiogenesis. When cancerous cells grow, travel to other parts and form tumor in other sites, it is termed as metastasis or secondary cancer as shown in Figure 1.2. Still, the name of original cancer retains even if it is spread to other parts of body. For instance, when lung cancer spreads to bones, it is termed as metastatic lung cancer even if the patient is only demonstrating symptoms of tumor in bones (John 2005; Mothoneos 2016).

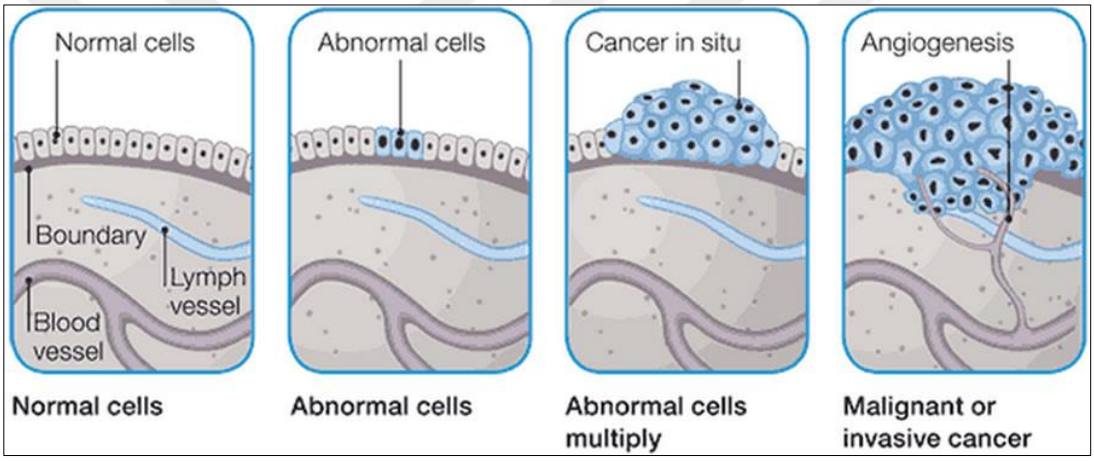

Figure 1.2. Schematic diagram shows the development and spread of cancer (Mothoneos 2016)

1.2.1. Lung Cancer

At present, lung cancer has proven to be the main cause of cancer related deaths all around the world. Every year, over 1.59 million deaths occur due to lung cancer. Only in 2012, around 1,590,000 individuals died of lung cancer. Mortality rates vary for males and females. This is because males tend to smoke more than females and smoking is major cause of lung cancer. The other reasons for lung cancer are include genetic factors, particle prolusion, hazardous chemicals and radon exposure. The reason behind high mortality rate of lung cancer is the fact that it is mostly diagnosed at advanced stage of the disease (Islami et al 2015; Sánchez-Valle et al 2017; Yagi et al 2017).

Lung cancer has proven to be a malignancy during which cancer grows in one or two lungs in uncontrolled manner. When cancer starts developing in the lungs, it is termed as primary lung cancer. However, it is capable of invading other regions like bones, liver, adrenal glands, brain and lymph nodes. It is also possible that cancer from any other part of the body invades the lungs. In this case, the disease is known as metastatic or secondary lung cancer (Mothoneos 2016). In particular, lung cancer initially develops due to unchecked multiplication of cells because of genetic damage in the cells. Distant parts of the body can also be affected by the lung cancer. Lung cancer may end up in death if not treated for example in the final stagetrouble the breathing and shortness of breath is very commonplace in people with advanced cancer, but it is able to be managed on the quit of lifestyles. The patient can feel short of breath and want to respire faster and tougher than ordinary. The patient might feel like that has liquid in his lungs and it makes him want to cough. In some cases, lung cancer is termed as bronchiogenic carcinoma or bronchiogenic cancer indicating cancer of bronchi which are airways to lungs. Majority of lung cancers start developing in cells that layer the bronchi (John 2005; Kalemkerian et al 2016).

1.2.2. Types of Lung Cancer

Site of origination of lung cancer is the epithelial cells present in the bronchi. In general, epithelial cells constitute the covering for free surfaces in the living system like airways. On the basis of their appearance under microscope, lung cancers are divided into some groups namely small cell lung cancer (SCLC) and non-small cell lung cancer (NSCLC), squamous cell carcinoma and adenocarcinoma. Around 80% lung cancers in the United States are NSCLC, this is just as an example. SCLC and NSCLC are two main types of lung cancers and differ in growth and spreading. Treatments for these two are also different (John 2005; Kalemkerian et al 2016).

1.2.2.1. Small Cell Lung Cancer

In case of SCLC, the cancerous epithelial cells are unusually small. For that reason, this cancer is also known as oat cell carcinoma indicating resemblance with the oat grains. It is also known as undifferentiated carcinoma. The term carcinoma generally indicates malignant tumors arising from epithelial cells. In some cases, SCLC cells appear as

spindle or polyglonal (multisided). Moreover, SCLC has been strongly related with tobacco smoking. Only 1% of SCLC patients are non-smokers. Growth of SCLC is quicker as compared to the NSCLC. SCLC usually metastasizes to different organs in the initial stages of the disease. Initially, SCLC proves to be responsive to radiation therapy and chemotherapy. SCLC usually develops in one of the two bronchi and tumors are mostly found at the center of the lung. The disease has mostly metastasized when it is diagnosed (John 2005; Kalemkerian et al 2016).

1.2.2.2. Non-Small Cell Lung Cancer

NSCLC has proven to be the common type of lung cancer as more than 80% of lung cancer patients have NSCLC. Owing to the efficient and advanced treatment approaches, prognosis and survival rate of NSCLC patients has demonstrated improvement in recent years. Still, treatment is challenged by the metastatic nature of the tumor. For that reason, researchers aim for studying the mechanisms involved in development of NSCLC and for identifying pharmaceutical agents which can impede with progression of cancer (Zhao et al 2017). NSCLC has been divided further into four kinds namely large cell carcinoma, Broncho-alveolar carcinoma, squamous cell carcinoma and adenocarcinoma. All these types of NSCLCs demonstrate similar growth and also have similar treatments. All these types of NSCLCs have variants or subtypes. Variants are named after peculiar growth pattern visible through microscopy (John 2005; Mothoneos 2016; Patient and Centre 2017).

1.2.3. Classification Pathological Staging and Grading in Lung Cancer

Identification of the exact stage of lung cancer is quite complicated. This is because the signs and symptoms of different stages tend to mix or overlap. Staging of cancer or finding out the extent to which cancer has spread is quite important for deciding the treatment strategy for a particular patient. Staging of SCLC and NSCLC is performed in a similar manner. The TNM system is used to determine the stage of cancer. Where T stands for tumor (site of origination and size of cancer); N stands for lymph node (filters in the living system that can allow spreading of cancer) and M stands for metastasis (sites invaded by cancer through mostly through blood stream). Based on these data, lung cancers are staged as I, II, III or IV. First two stages are referred to as early stage cancer

and usually include T1-2 N0-1 M0 tumors. Third stage is termed as locally advanced lung cancer and includes TN2-3 M0 tumors. Finally, fourth stage is known as advanced or metastatic cancer and includes any T N M1 tumors. In case of advanced cancer, the cancer has spread from lung and lymph nodes nearby (Mothoneos 2016; Patient and Centre 2017).

1.3. Programmed Cell Death

Programmed cell death (PCD) is an essential cellular process which is crucial not only for removal of worn out cells but also for maintenance of tissue homeostasis and development. It is because of this process that a balance is maintained between multiplication and death of cells. Diseases like cancer can be encountered if this balance is disturbed. Moreover, fate of cancer cell is also affected by this process. Cells with variable phenotypes are seen during this process which influences the nucleus, cellular membranes and organelles. Researchers have developed numerous nomenclature systems for classification of PCD. Three main cell morphologies for PCD have been illustrated in a well-established classification system. In this system, PCD is classified as Type I (apoptosis), Type II (autophagy) and Type III (programmed necrosis). These types can be identified simply on the basis of morphological features (Ouyang et al 2012; Sun and Peng 2009).

In case of multicellular living systems, each cell is a member of a cellular community which is quite complicated but very organized. Population of cells is strictly controlled not only by regulating division of cells but also the death of cells. When certain cells are not required any more, they trigger intracellular death program to commit suicide. For that reason, this phenomenon is termed as programmed cell death (Alberts 2002).

1.3.1. Apoptosis

Apoptosis refers to a process during which a cell itself decides that it is going to die. This process takes place in multicellular organisms and is mostly for the betterment of the organism on the whole. This often occurs for the greater good of the whole organism, such as when the DNA of cell has become damaged and it may become cancerous (Lowe and Lin 2000). Apoptosis can be considered as a repair and quality control strategy as senescent cells, genetically damaged or unwanted cells get eliminated. Accordingly,

apoptosis is of crucial importance for the growth and development of higher organisms. This mechanism of cell death is highly conserved in animals as well as plants and is thoroughly studied biochemically as well as genetically. During apoptosis, intracellular proteases including caspases and internucleosomal DNA fragmentation are activated. Besides these, molecules expressed on cell surface get altered thereby allowing quick recognition and phagocytosis of cells. In this way, several cells are quickly eliminated from a tissue. Hence, apoptosis can be seen as a mechanism for organized removal of cells without causing inflammation (Su et al 2013; Sun and Peng 2009).

Kerr et al. (Kerr et al 1972) illustrated the process of type I PCD i.e. apoptosis for the first time. The researchers characterized the process with peculiar changes in the morphology and biochemistry of the cells undergoing apoptosis. Morphological changes include shrinkage of cell, fragmentation and condensation of nucleus, loss of adhesion with extracellular matrix (ECM) or nearby cells and dynamic membrane blebbing (Nishida et al 2008). Biochemically, chromosomal DNA gets cleaved into internucleosomal fragments, cleavage of numerous intracellular substrates through proteolysis occurs specifically and phosphatidylserine is externalized (Ouyang et al 2012).

1.3.1.1. Apoptosis and Cancer

Apoptosis has been found to be involved in preventing and causing certain clinical conditions. Cancer in humans is prevented by apoptosis as it makes the cells carrying defected DNA to die prior to development of cancer.

The chief role played by apoptosis is elimination of cells which can be harmful for the entire living system. Apoptosis usually occurs as soon as a cell finds that its DNA is damaged to the extent that it cannot be repaired. DNA damage in such cases causes activation of apoptotic mechanism thereby preventing development of cancer. Yet, this may not occur in all cases and activation of apoptosis may fail. In particular, this occurs when genes needed for apoptosis are affected by the DNA damage. Designing and development of drugs for cancer is challenged by the fact that the drug should induce apoptosis only in cancerous cells. A drug that makes both cancerous and normal cells to die can be very hazardous. It is worth mentioning that cancer may not necessarily occur due to failure of apoptotic pathway. Researchers have found that cancers may develop in

cells which are more prone to apoptosis; however, it seems that these cells are made to ignore signals for apoptosis and continue to live with the damaged DNA. It has also been found that cancerous cells which are eliminated through medication usually die through apoptotic pathway implicating that cells which can ignore apoptotic signals and make themselves apoptosis resistant are also resistant to treatment. However, treatment of cancer is the subject yet to be studied further and exploration of apoptosis can bring to light new opportunities for cancer treatment (Lowe and Lin 2000; Ouyang et al 2012).

1.3.1.2. Apoptosis Pathway

Apoptosis occurs through two main pathways. These pathways have different means for activation of the process and both have their own significance.

1.3.1.2.1. Extrinsic Pathway

Extrinsic pathway for apoptosis is characterized by reception of an extracellular signal which induces PCD in the cell. Diseased or unwanted cells can be eliminated through this pathway. This complicated pathway can be divided into following steps shown in Figure 1.3. Certain molecules or expression of certain genes can cause down regulation or upregulation of these steps. Step 1: The extrinsic pathway initiates when an external signal entity binds with the receptor expressed on the cell surface. FAS and TNF-Related Apoptosis-Inducing Ligand (TRAIL) have been reported to be the most common molecules which stimulate the activation of extrinsic pathway. It is possible that nearby cells release these molecules when certain cells are not required or damaged. FAS binds specifically with the FAS Receptor (FASR) and TRAIL binds with the TRAIL receptor (TRAILR). Just like other receptors of signaling mechanisms, the FASR and TRAILR tend to bind with the ligand as soon as they encounter them. Binding of the receptor with the ligand is followed by changes in the intracellular domain of the receptor. Step 2: An intracellular protein the Fas-associated death domain adapter protein (FADD) gets changed when the intracellular domain of FASR or TRAILR is changed. Intriguingly, FADD means FAS-Associated Death Domain protein Activation of the FADD protein is followed by its interaction with two other proteins that cause initiation of the PCD. Step 3: The Pro-caspase-8 and the pro-caspase-10 are found inside the cell in inactive form. When activated FADD interacts with these proteins, they get activated. However, when

an activated FADD faces the abovementioned two molecules, the protein component which retains inactivity of these proteins include the cleaved or cut away parts.

The pro-caspases then become caspase-8 and caspase-10 that have been referred to the beginning of the end cell due to their role in starting apoptosis. The Caspase-8 and Caspase-10 spread in the cytoplasm and cause many other cellular molecules to get changed. For instance, messengers which initiate breakdown of DNA are triggered by Caspases. Step 4: Activated Caspases also cause activation of BID molecule to give rise to tBID molecule. When a particular component of BID is removed from the BID, it is converted into tBID. Once tBID is formed, it travels to the mitochondria where it causes activation of BAK and BAX. This is the step which is common in extrinsic and intrinsic pathway of apoptosis. Steps 1-4 described above only occur in the extrinsic pathway. Steps after the activation of BAK and BAX are same in both pathways. Accordingly, steps 3-7 of the intrinsic pathway can be considered as steps 5-9 of the extrinsic mechanism (Elmore 2007; Sun and Peng 2009).

1.3.1.2.2. Intrinsic Pathway

Step 1: Any damage to cell or stress stimulates the intrinsic pathway of apoptosis. Deficiency of oxygen, DNA damage and other stress factors negatively influence the capability of the cell to perform its activities. Accordingly, a cell under stress decides to discontinue its survival. Consequently, a group of proteins known as BH3-only proteins are activated. Step 2: BH3-only proteins refer to a protein group that comprises of numerous pro and anti-apoptotic proteins. Activation of these proteins determines whether apoptotic pathway is activated or inactivated. Step 3: A state termed as Mitochondrial Outer Membrane Permeabilization (MOMP) is induced by activation of BAX and BAK. The term MOMP means mitochondrial outer membrane permeability and is viewed as the point of no return for apoptosis. Although the changes resulting in MOMP activation can be halted by using inhibitors; however, once this state has been induced, the cell will eventually die. This condition results in cell death by permitting discharge of cytochrome C in cytoplasm. Step 4: The cytochrome C performs crucial part in the mitochondrial electron transport chain under normal physiological conditions. Nevertheless, the cytochrome C molecule can be released from mitochondria during MOMP and inside the cytoplasm it may behave as a signaling entity. In particular, the

cytochrome-C present in cytoplasm stimulates the development of the ominous-sounding apoptosome. A set of proteins, APAF1, form this apoptosome and these proteins cause initiation of the breakdown of the cell. Step 5: As soon as the apoptosome is formed, the pro-caspase-9 is converted to form Caspase-9. The Caspase-9 can cause several changes in the cell just like the Caspase-8 and Caspase-10 cause in the extrinsic pathway. Step 6: The protein Caspase-9 is capable of performing numerous activities leading to apoptosis. An important activity performed by this molecule is that it activates Caspases 3 and 7. Step 7: As soon as the Caspases 3 and 7 are activated, they cause dissociation of different cellular structures. For instance, Caspase-3 condenses and results in dissociation of DNA of the cell (Elmore 2007; Sun and Peng 2009).

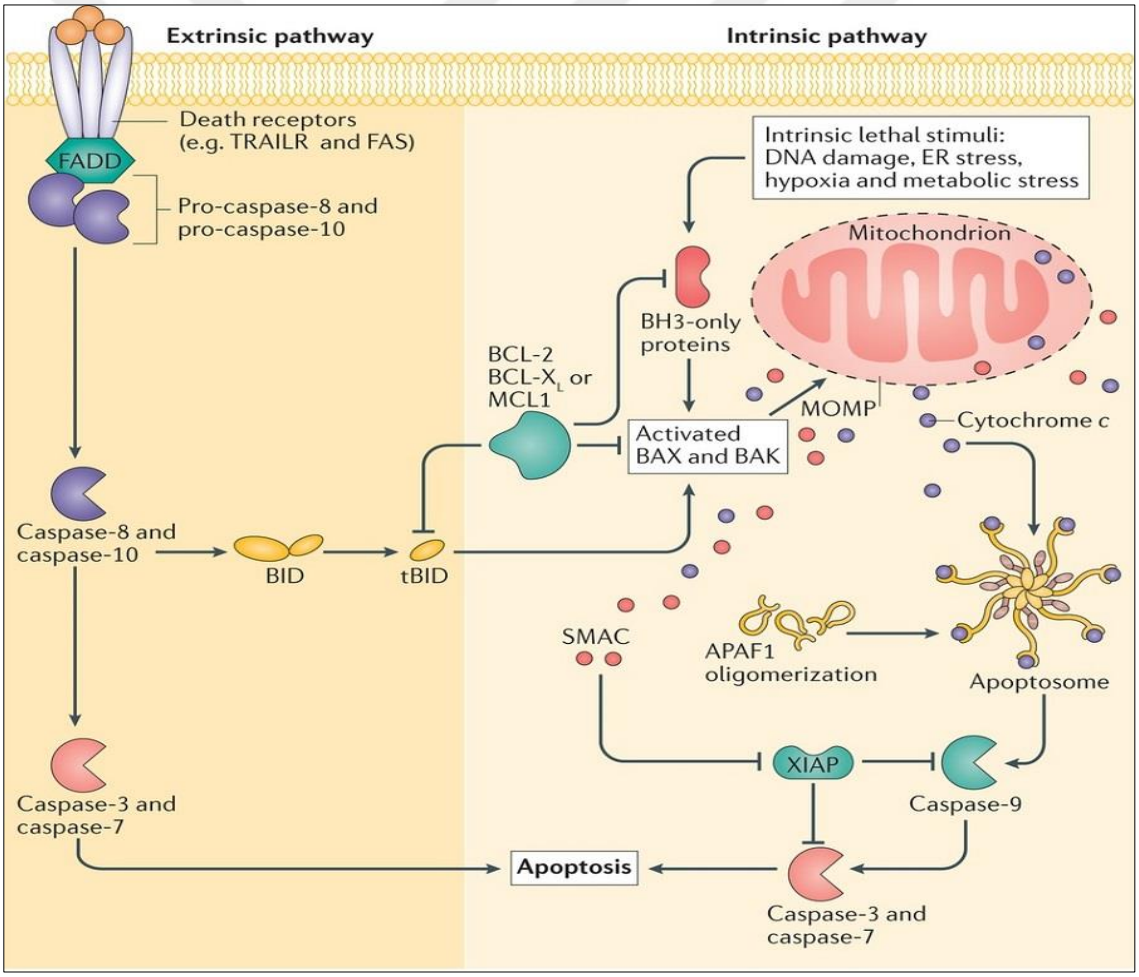

Figure 1.3. Schematic representations of apoptotic events. The two main pathways of apoptosis are extrinsic and intrinsic pathway. Each requires specific triggering signals to begin an energy-dependent cascade of molecular events. Each pathway activates its own initiator Caspase (8, 9, 10) which in turn will activate the executioner Caspase-3 (Lowe and Lin 2000)

1.3.2. Autophagy

Autophagy has proven to be the main catabolic mechanism in eukaryotic cells for recovering basic molecules and for sustaining sufficient quantities of amino acids for protein synthesis especially during food deficiency. Researchers have found that this process is crucial for turnover of different macromolecules and proteins (Maiuri et al 2007b). The term "Autophagy" is derived from Greek word that means "self-eating". Christian deDuve used this term for the first time about 40 years ago. His description of the term was mainly due to the observation that when rat liver was perfused with glucagon (pancreatic hormone), the mitochondria and other intra-cellular components are degraded inside the lysosome (Deter and De Duve 1967; Glick et al 2010). In general, autophagy signifies breakdown of cytoplasmic structures inside the lysosomal compartment (Klionsky 2005; Mizushima 2007). It is worth mentioning that autophagy is totally different from the breakdown of extracellular and membranous structures inside the lysosome after endocytosis. Autophagy is carried out by a peculiar structure known as autophagosome. Since a part of cytoplasm is engulfed by the autophagosome, autophagy seems to be a nonselective mechanism for degradation (Mizushima 2007; Su et al 2013). Surprisingly, this catabolic phenomenon is conserved in the evolutionary tree. It starts with the development of autophagosome which is a structure enveloped by two membranes. This structure carries organelles and macromolecules which are meant for degradation (Chen et al 2010; Huett et al 2010; Li et al 2011; Liu et al 2011). Characteristic features of autophagy include dilation of mitochondria, detailed remodeling of intracellular membrane and development of autophagosomes. Fusion of autophagosomes with the lysosomes results in formation of autolysosomes – structure demonstrating digestion of sequestered parts of cell (Reggiori and Klionsky 2005). Degradation of cellular components leads to production of amino acids and fatty acids which can be utilized for protein synthesis or oxidized by electron transport chain resulting in generation of ATP especially under conditions of nutrient deficiency (He and Klionsky 2009; Levine and Yuan 2005). Still, reports indicate that cells demonstrating autophagy can undergo death and this differs from programmed necrosis and apoptosis. In contrast to apoptosis that involves Caspases activation resulting in dissociation of proteins (Luthi and Martin 2007), death of autophagic cell involves buildup of autophagic vesicles in huge numbers. During initial stages of the process, organelles are degraded. In

contrast to this, structural and functional integrity of cytoskeleton is retained till later stages (Reggiori and Klionsky 2005). Death of autophagic cell may also involve morphological changes like membrane blebbing or condensation of chromatin. However, this particular pathway of cell death lacks development of apoptotic bodies and DNA fragmentation (He and Klionsky 2009). Researchers have detected more than thirty ATG genes in yeast. Orthologs of at least 11 of these genes (ATG1, 3, 4, 5, 6, 7, 8, 10, 12 and 16) are found in mammals. In case of mammals, ATG6 and ATG8 are known as BECN1 and LC3 (Bialik et al 2010; Eisenberg-Lerner et al 2009; Ouyang et al 2012; Sun and Peng 2009).

There are three different types of autophagy. These are microautophagy, macroautophagy and chaperone mediated autophagy (CMA). These are classified on the basis of means of cargo delivery to lysosomes (Sun and Peng 2008). Chief autophagic pathway is the macroautophagy which involves transportation of cytoplasmic contents to the lysosome via autophagosome. The autophagosome is an intermediary entity surrounded by two membranes. Fusion of autophagosome with the lysosome results in formation of autolysosome. Conversely, in case of microautophagy, the cytoplasmic structure meant for dissociation is directly taken in by the lysosome via an invagination. This particular mechanism plays crucial role in sustaining size of organelle, membrane homeostasis and endurance of cell during nitrogen deficiency (Li et al 2012). During chaperone-mediated autophagy (CMA), cytoplasmic proteins are transported directly to the lysosomal membrane through a complex containing chaperone proteins. The lysosomal membrane receptor LAMP-2A (lysosomal-associated membrane protein 2A) recognizes the chaperone proteins and binding of these two leads to unfolding and degradation of the complex (Glick et al 2010; Klionsky 2005).

1.3.2.1. Basic Autophagy Machinery

The process of autophagy starts with an isolation membrane as shown in figure 1.4. This membrane isolation membrane is also termed as phagophore which probably originates from the lipid bilayer given by the trans-Golgi complex and/or endoplasmic reticulum and endosomes (Axe et al 2008; Simonsen and Tooze 2009). Yet, the source of mammalian phagophore still needs to be confirmed. Expansion of phagophore allows engulfment of cytoplasmic cargo like ribosomes, organelles and protein aggregates. In

this way the unwanted components are sequestered in a double-membrane structure (Mizushima 2007). This autophagosome carrying the cargo fuses with the lysosome permitting the dissociation of cargo contents by acid proteases from lysosome. The amino acids and other products generated by the dissociation of cargo are sent to cytoplasm for usage by permeases and transporters found in lysosome (Mizushima 2007). Hence, autophagy is not only significant because it causes elimination of damaged or unwanted components but also plays the role of recycling factory by recovering the basic building blocks which can be used for synthesis of biochemical entities or for metabolism(Glick et al 2010).

Certain signaling pathways regulate the process of autophagy. For instance, stress-signaling kinases like JNK-1 encourage autophagy through Bcl-2 phosphorylation and in this way facilitate interaction between VPS34 and Beclin-1 (Wei et al 2008). The main signaling entity regulating the extent of autophagy in cells is possibly the mTOR kinase which probably influences autophagy by inhibiting the ATG1/Ulk-1/-2 complexes during initial phases of formation of phagophore (Xie and Klionsky 2007). Surprisingly, mTOR is the entity which regulates the processes of autophagy as well as growth. Down regulation of autophagy is mediated by mTOR during conditions with nutrient sufficiency. mTOR also triggers growth promoting processes like translation of proteins (Diaz-Troya et al 2008). Reduced concentration of ATP in cytoplasm and hypoxia induces the process of autophagy while the mTOR activity is inhibited via decreased activity of Rheb GTPase. On the other hand, the process of autophagy is prevented by amplified growth factor signaling using insulin receptor plus its adaptor IRS1 and other growth factor receptors which cause activation of PI3-kinases Class I and Akt in order to encourage mTOR activity by inhibiting TSC1/TSC2 and amplifying activity of Rheb GTPase (Diaz-Troya et al 2008; Sabatini 2006).

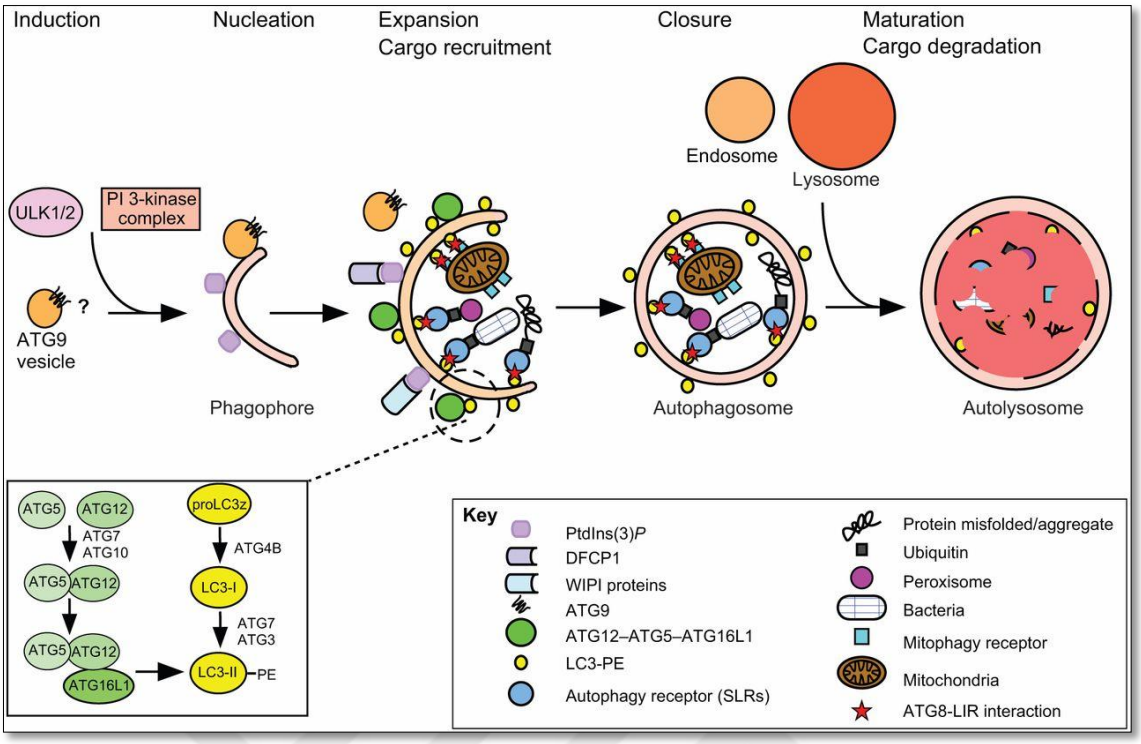

Figure 1.4. Molecular entities and mechanisms that regulate autophagy. Autophagy can be viewed as a complicated self-degradative phenomenon which involves steps described below. Induction and Nucleation: Regulated development of phagophore at ER and other membranes by Beclin-1VPS34 under stress conditions; conjugation of Atg5-12 followed by association with Atg16L and multimerization; Expansion: processing of LC3 followed by its insertion in the extended membrane of phagophore. Closure: Engulfment of specific or random entities meant for degradation while the LC3-IIATG8 gets recycled by ATG4. Maturation: Joining of the autophagosome and lysosome resulting in degradation of inserted components by lysosomal proteases (Birgisdottir et al 2013)

1.3.2.2. Autophagy and Cancer

The main catabolic mechanism which demonstrates connections with the phenomena taking place in cancerous cells is autophagy. It is highly regulated process controlled by certain autophagy-related genes (ATGs). This important pathway occurs in response to intra- or extra-cellular stress and may end up with continuation of cell survival. Yet, when over-activated, autophagy leads to death of cell (Wang et al 2011). A considerable challenge encountered while examining the link between autophagy and cancer is to find out if autophagy is promoting survival of cell or playing its role in death of cell. Role of autophagy in protecting survival of cell under stress conditions has been established. Under nutrient depleted conditions, breakdown of different cytoplasmic components serve as a source of basic molecules and energy which is needed for cell survival (White 2012). For that reason, activation of autophagy can contribute in protecting survival of

cell during initial stages of cancer (Kundu and Thompson 2008). Conversely, autophagy may act as a tumor suppressor as it causes blockage of anti-autophagic genes and activation of pro-autophagic genes during the course of oncogenesis. In contrast to this, it can also play pro-tumor role through regulation of several mechanisms that involve p53, mTORC1C2, Class III and I PI3K, Beclin-1 and Bcl-2 (Ouyang et al 2012). It is worth mentioning that this complex process involves contribution of several upstream regulatory signaling mechanisms (Morselli et al 2009). Even though the regulatory pathways for autophagy are not completely deciphered; the exact role of this process in cancer remains questionable. This is because it is hard to analyze if autophagy is playing its role for death or survival of cell (Gozuacik and Kimchi 2004; Liu et al 2013).

1.3.2.2.1. Autophagy as Tumor Suppressor

Any disturbance in autophagy causes buildup of damaged or unwanted entities especially mitochondria thereby causing genome instability, DNA damage and oxidative stress which are already established as factors leading to initiation and progression of cancer (Chen and Karantza 2011; Levine and Klionsky 2004; White 2015). Accordingly, researchers have found association between autophagic defects and the accumulation of oncogenic mutations and increase vulnerability for tumor (Choi 2012; Karantza-Wadsworth et al 2007; Mathew et al 2007).

Earlier, autophagy was considered to be a tumor-suppressing pathway. This has been strongly supported by the reports concerning Bcl-2-interacting protein Beclin 1 (BECN1 or ATG6). Researchers have frequently found monoallelic deletion of Beclin 1 in various cancers like human breast cancer (Futreal et al 1992), ovarian cancer (Aita et al 1999) and prostate cancer (Gao et al 1995). Similarly, increased rate of liver cancer, lung cancer and lymphoma has been found in mice having disrupted Beclin 1 gene (Qu et al 2003; Yue et al 2003).

It has been demonstrated that several tumor suppressor proteins promote autophagy. These include Atg4c (Marino et al 2007), Bax interacting factor-1 (Bif-1) (Takahashi et al 2007), BH3-only proteins (Maiuri et al 2007a) DAPkinase (Bialik and Kimchi 2010), LKB1(Liang et al 2007), ultraviolet radiation resistance-associated gene (UVRAG) (Liang et al 2006), PTEN (Arico et al 2001), TSC (Zhou et al 2009), nuclear p53 (Maiuri

et al 2010) and AMPK (Luo et al 2010). Taken together, these evidences point towards tumor-suppressing role of autophagy and indicate that autophagy can be viewed as a characteristic feature of cancer overcome (Choi 2012; Hanahan and Weinberg 2011).

1.3.2.2.2. Autophagy as Tumor Promoter

Main function of autophagy in cancerous cells is to make cell tolerant to stress thereby promoting survival of cell (Degenhardt et al 2006). Owing to greater rate of cellular division, cancer cells demonstrate greater metabolic demands (Mathew et al 2009). Autophagy can be activated by metabolic and cytotoxic stress factors like nutrient deficiency and hypoxia so that macromolecules could be synthesized and energy could be generated. In hypoxic tumor cells, induction of autophagy occurs from parts which are at distance from blood vessels. Moreover, this autophagy can be amplified by expression of HIF-1α expression. Expression of angiogenic factors like nitric oxide synthase (NOS), platelet derived growth factor (PGDG) and vascular endothelial growth factor (VEGF) is also amplified by HIF-1α (Egan et al 2011). Researchers have demonstrated inhibition of cell growth by suppression of important autophagy proteins in a group of these cells implicating that autophagy is involved in sustaining survival of tumor cell (Yang et al 2011).

Physiological role played by autophagy concerns with the preservation of the cellular homeostasis when cell is experiencing any stress. In agreement with this is the fact that cancerous cells may use autophagy as a strategy for survival in response to stress factors like acidic and hypoxic microenvironment. Similarly, certain cancerous cells can utilize autophagy for adapting themselves with the metabolically stressful, nutrient deficient and hypoxic microenvironment and also with the stress induced the therapeutics (Rouschop and Wouters 2009). Researchers have reported induction of autophagy in human cancer cell lines in response to antiestrogen hormonal therapy (like tamoxifen), radiation therapy, chemotherapy (like etoposide, temozolomide, doxorubicin) histone deaceltylase inhibitors, rapamycin, imatinib, arsenic trioxide, TNFα and TNFγ (Kondo et al 2005). Such evidences are in favor of the proposition that these therapies cause induction of autophagy which is pro-survival and protective thereby amplifying the resistance of cell to such therapies. Accordingly, discontinuation of autophagy can result in amplified cell death and cessation of growth of tumor (Dalby et al 2010).

A crucial requirement of cancerous cells is that their metabolism is adapted in a way that it can fulfill the requirements of increased cell division. Accordingly, signaling mechanisms that regulate metabolism are influenced by oncogenes thereby promoting proliferation and cancer growth (Jiang and DeBerardinis 2012). During progression of cancer, activation of autophagy occurs as a consequence of several stress factors like ER stress, nutrient deficiency and hypoxia (Mathew and White 2011). If somehow autophagy is inhibited when cell is experiencing metabolic stress, apoptosis will be amplified resulting in decreased progression of tumor. This section describes the effect of regulating autophagy on growth of tumor (Janku et al 2011). Owing to insufficient blood supply and defected angiogenesis, tumor cells experience increased metabolic stresses like scarcity of oxygen and nutrient deficiency. Amplified hypoxia causes changes in metabolism, resistance to therapies and improved invasiveness. Tumor cells experience metabolic stress largely due to the fact that they have increased metabolic requirements for cell division (Vander Heiden 2011). In such stressed cells, autophagy serves as a source of nutrients and energy thereby supporting survival of tumor cell in hypoxic conditions. According to researchers, activation of autophagy is one of the most prominent activities of tumor cells in response to stress (Lum et al 2005; Mathew et al 2009; White and DiPaola 2009).

1.3.2.3. Autophagy as a Program Cell Death

It has been established that anticancer therapies induce cell death mainly through necrosis and apoptosis (PCD-type-I). Necrosis is the dying of most or all the cells in an organ or tissue because of disease, damage, or failure of the blood deliver (Edinger and Thompson 2004). Apoptosis has largely been viewed as a synonym for programmed cell death and was considered to be the main pathways causing death of cells treated by radiation and chemotherapy. Researchers have recently established that programmed cell death may occur through mechanism other than apoptosis. These days, autophagic cell death is known as programmed cell death type II. Unlike apoptosis, cell death through autophagy lacks DNA laddering, is independent of Caspases and involves increased autophagic breakdown of damaged or unwanted cellular components (Dalby et al 2010; Kirisako et al 1999). In particular, researchers have described autophagic cell death as a type of PCD in which cell death occurs only through autophagy. According to reports, cell death is said to be autophagic only if:

1. Cell death is caused in absence of apoptosis.
2. Dying cell demonstrates amplified autophagic flux instead of autophagic markers only.
3. The dying cell can be rescued through inhibition of autophagy by genetic and pharmacological inhibitors.

Besides the cell protective role played by autophagy which has been reported by significant research, occurrence of cell death through autophagy has also been studied and autophagy has been established as a mean for cell death provided that the dying cells demonstrate the autophagic characteristics. Researchers have demonstrated autophagy leading to non-apoptotic cell death in cancer cells (Kanzawa et al 2005; Shao et al 2004; Shen and Codogno 2011). As mentioned earlier, long-lasting stress together with increased autophagy can end up with cell death provided the turnover of organelles and proteins is less than the requirement of cell. Type of cell and its genetic makeup determines whether anticancer drugs will or will not induce the autophagic cell death. Autophagy has been shown to be induced by STF-62247 (a novel small molecule) in VHL deficient renal cell carcinoma cells leading to cell death (Turcotte et al 2008). Nevertheless, there is scarcity of in vivo studies regarding this and researchers need to determine if autophagic cell death can be induced in tumor cells through anticancer therapeutics (Yang et al 2011).

1.3.3. Crosstalk between Apoptosis and Autophagy

Apoptosis and autophagy are well-controlled processes, and they have a complex crosstalk together because they may cooperate antagonise or help each other. They are activated in response to energy metabolism, growth factor depletion, starvation (Nikoletopoulou et al 2013). They have a distinct morphological characteristic and physical process, but they existcomplicated interrelationships together. They able to exert synergetic effects or autophagy activated only when apoptosis suppressed (Ouyang et al 2012). For example, in gliomas cells the pro-survival effects of autophagy against apoptotic cell death were identified (Chang et al 2014).

The autophagy may withstand during the loss of extrinsic signals that maintain nutrients and energy metabolism for extracellular matrix (ECM)-disrupted cells, results to delay the apoptosis and providing the additional time to cells re-attach to a suitable ECM. The

autophagy may support the survival of hepatocellular carcinoma (HCC) through the activation of mitochondrial B-oxidation and intracellular ATP production under hypoxic condition. Accumulating evidence proposes that autophagy also supplies a mechanism for matrix-detached pre-metastatic tumor cells to avoid die (Su et al 2015). Briefly, Apoptosis is a closely regulated process of removing damaged and unwanted cells, while autophagy is a pathway of cellular catabolic process that is included in lysosomal degradation and recycling of organelles and proteins, and pointed as an important role for survival / protective mechanism for cancer cells in response to chemotherapy or metabolic stress. Whereas, the relationship between autophagy and apoptosis has not been characterized in detail and not well understood (El-Khattouti et al 2013).

1.4. TP53-Induced Glycolysis and Apoptosis Regulator

Expression of the c12orf5 gene results in production of TIGAR protein. Jen and Cheung found this gene during their computerized search for the novel p53-regulated genes that get switched on in response to ionizing radiation (Jen and Cheung 2005). Karim Ben Saad and his colleague (2006) carried out a research on structural and functional characteristics of c12orf5 gene and named it as TIGAR gene where TIGAR stands for TP53-induced glycolysis and apoptosis regulator. This gene is located on chromosome 12p13-3. There are two potential binding sites for P53. BS2 is within the first intron and BS1 is located upstream of the first exon. BS1 demonstrate high binding affinity for p53 whereas BS2 demonstrates low binding affinity. Besides these, there are six coding exons in this gene (Bensaad et al 2006).

The TIGAR protein protects the cell from the harsh effects of reactive oxygen species especially the DNA damage as it reduces the concentration of ROS. It also offers protection against apoptosis induced by DNA damage. Production of TIGAR protein results in reduction in concentration of fructose-2, 6-bisphosphate (Fru-2, 6-P2) and amplification of glucose-6-phosphate dehydrogenase (G6PD) levels leading to pentose phosphate shunts resulting in generation of ribose-5-phosphate and NADPH. This causes glycolysis to be inhibited which is important for DNA repair and synthesis of nucleotides (Bensaad et al 2006; Cheung et al 2012; Li et al 2014; Lui et al 2011; Xie et al 2014; Yin et al 2014). Researchers have found increased levels of TIGAR protein in different

cancers like breast (Won et al 2012) and colorectal cancers and human glioblastoma (Wanka et al 2012; Xie et al 2014).

According to previous study by Bensaad and his colleagues, fall in TIGAR protein levels was shown to accompany the switch to apoptosis in cells. So this is a good evidence that provide an important role of TIGAR protein in apoptosis (Bensaad et al 2006).In another study, there results demonstrated that TIGAR inhibits both apoptosis and autophagy after silencing that protein in human hepatocellular carcinoma (Xie et al 2014). Taken together, these studies are a good evidence for role TIGAR in apoptosis and autophagy.

1.5. Oxidative Stress and Cancer

1.5.1. NADPH Oxidase

NADPH oxidase is a membrane bound enzyme complex present in cell membrane and in phagosomal membrane utilized by neutrophils for engulfing microbes. NOX1, NOX2, NOX3 and NOX4 are the isoforms of this enzyme. It is responsible for transporting electrons across the boundary of phagocytic vacuole constituting superoxide in the lumen. It has been established that this enzyme complex causes death of microbes by producing reactive oxygen species and via myeloperoxidase activity (Sahoo et al 2016). Superoxide is produced by NADPH oxidase when it transfers intracellular electrons across the membrane and donating these electrons to molecular oxygen resulting in formation of superoxide anion. This reactive radical can be generated in phagosomes carrying engulfed fungi and bacteria; alternatively, it can be generated outside the cell. Superoxide can produce hydrogen peroxide inside the phagosome which will eventually produce reactive oxygen species after certain reactions (Skonieczna et al 2017).

1.5.2. Reactive Oxygen Species

ROS refer to a group of reactive molecules containing oxygen. These include oxygen anions, hydrogen peroxide and free radicals of oxygen. In general, these small short lived species are extremely reactive (Li et al 2015; Rahal et al 2014). ROS are produced from two main sources. These are NADPH oxidase (NOX) and mitochondria. Mitochondria generate ROS as respiratory by-product; whereas NADPH oxidase generates superoxide via membranes of neutrophils and phagosomes (Li et al 2015; Scherz-Shouval and Elazar

2011). These reactive oxygen species are capable of oxidizing and damaging mitochondrial products like lipids, amino acid precursors and nucleic acids. As a result, mitochondrial dysfunction can be induced leading to oxidative stress (Li et al 2015; Scherz-Shouval and Elazar 2007). Under normal physiological conditions, moderate concentrations of ROS act as signals required for cell survival and proliferation. However, amplified levels of ROS may cause cell death. For that reason, the cell maintains a balance between production and removal of these reactive species.

ROS are being continuously produced in the living system as they are needed for regulatory mechanisms. They may also cause certain clinical conditions like cancer. Researchers have reported that ROS may work for promotion and suppression of cancer cell survival. 1) ROS act as regulators working for all steps of tumor development like transformation, survival, proliferation, invasion, metastasis and angiogenesis. 2) ROS also regulates chronic inflammation which is one of the main mediators of cancer. 3) Signaling molecules needed for progression of cell cycle are also regulated by ROS. 4) ROS control the expression of different tumor suppressor genes. 5) Increased concentration of ROS may cause suppression of tumor growth via prolonged activation of inhibitors of cell cycle. 6) Majority of the radio therapeutic and chemotherapeutic agents in use these days kill tumors through amplifying ROS. Considering these evidences, different cancer treatment strategies have been devised that involve amplification or elimination of ROS (Prasad et al 2016).

1.5.3. NFκB Pathway

It was discovered by Sen and Baltimore since 1986 (Siomek 2012). NF-κB incorporates a central importance in immunity and inflammation, additionally plays necessary roles in different processes, such as cell growth, survival and development, and proliferation, and features a role in several pathological conditions (Morgan and Liu 2011). Rift valley fever virus (RVFV) infected animal tissue cells and ends up in a rise in ROS that related with activation of NFκB (p65) and p53 responses (Narayanan et al 2014). While, in another study recommended raised ROS levels and reduced NF-κB activity after knockdown of termed thioredoxin-like 2 (TXNL2) in human carcinoma cell lines (Qu et al 2011). These are telling us there is interference between reactive oxygen species expression and NF-κB signaling.

NF-κB pathway could be activated via two main ways named the canonical and the noncanonical pathway, respectively (Oliver et al 2009) as shown in the figure 1.5. Some studies have demonstrated another way, so that we can also consider three ways of NF-κB activation: the classical, atypical and alternative pathway (Siomek 2012). The canonical NF-κB pathway has been outlined primarily in response to TNFα and interleukin(IL-1) signaling, prototypal pro-inflammatory cytokines that have necessary roles within the pathologic process of chronic inflammatory diseases for example inflammatory bowel disease (IBD), chronic obstructive pulmonary disease (COPD), asthma, and rheumatoid arthrtitis (RA) (Lawrence 2009). The alternative NF-κB pathway is identified by the inducible phosphorylation of p100 by Inhibitory Kappa B Kinase α (IKKα), resulting in activation of Nuclear Factor Kappa-Light-Chain-Enhancer of Activated B Cells (RelB/p52) heterodimers. The upstream kinase that activates IKKα during this pathway has been known as associate degree NIK (NF-κB causing kinase) (Senftleben et al 2001).

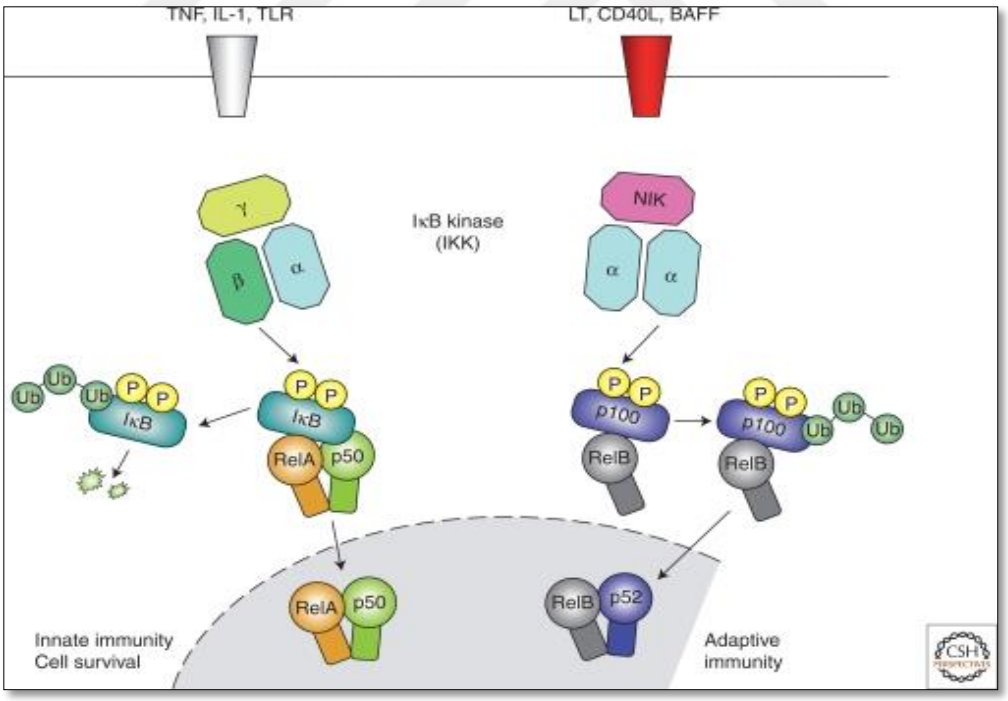

Figure 1.5. NF-κB pathways. This figure shows both of the pathways for NF-κB activation canonical and alternative (Lawrence 2009)

1.5.4. HO-1 Pathway

It was discovered since 1968 (Tenhunen et al 1969).The inducible variety of Heme Oxygenase-1(HO-1) could be a major endoplasmic reticulum (ER) associated heme protein and identified to plays necessary roles in protection against chemical and oxidative stress by degrading free heme discharged from degradation of heme proteins (Bansal et al 2014). Studies recommend the contribution of chemical stress, oxidative stress and ROS inducement the expression of HO-1 (Bindu et al 2011). And it is raised to stop DNA harm caused by the ROS, HO-1 down regulation results in the rise of DNA damage and ROS in cells (Lin et al 2013).

Signaling pathway of HO-1 is induced by oxidative stress for example green arrows show an elevation of HO-1 expression as shown in the figure 1.6. Red blocked lines show decreased level of expression. Several nitric oxide (NO) in different biological systems and can control the increased production of HO-1 as highlighted in the green box, are known inducers of HO-1, as well as hemoglobin/heme via the cluster of designation (CD163) receptor and lipopolysaccharide (LPS)via the toll-like receptors (TLR4) receptor. Anti-inflammatory cytokines are identified in blue; pro-inflammatory cytokines are highlighted in red. There are many cytokine signaling loops that include HO-1 activity, including a negative feedback loop between HO-1 and TNF-α (pro-inflammatory) and a positive feedback loop between HO-1 and IL-10 (anti-inflammatory). HO-1 can also bind to some transcription factors promoter (HMOX1 is the gene symbol for HO-1), alsonuclear factor erythroid 2–related factor 2(NRF2) at the antioxidant response element (ARE) site, but notably activator protein 1 (AP-1), cAMP response element binding (CREB), and NF-κB can bind to the promoter at independent binding sites and enhance HO-1 activity and expression (Ambegaokar and Kolson 2014).

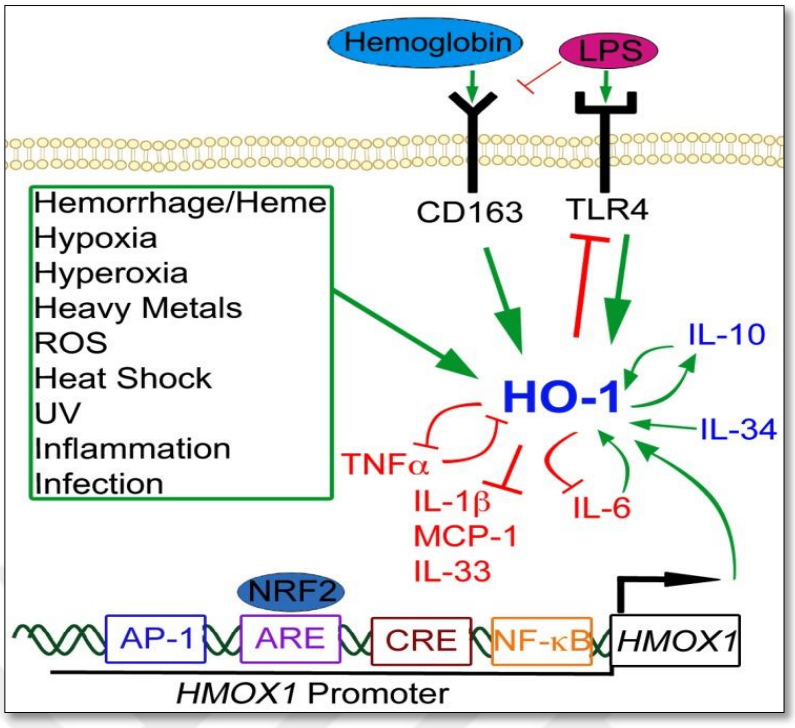

Figure 1.6. It shows the HO-1 pathways (Ambegaokar and Kolson 2014)

1.5.5. Oxidative Stress and Apoptosis

For the normal functioning and survival of most multi-cellular organisms, apoptosis is necessary. It is recently observed that apoptosis can be divided into at least three functionally distinct phases, i.e. induction, effector and execution phase. Recent studies have illustrated that ROS and the resulting oxidative stress play an important role in apoptosis. Different types of antioxidants can delay or block apoptosis. So, oxidative stress can be part of signal transduction pathway during apoptosis. Several essential players of apoptosis, including cytochrome C, pro-caspases, apoptosis-inducing factor (AIF), and APAF-1 are released into the cytosol during mitochondrial dysfunction. Taken together, elevating evidences give a support that oxidative stress and apoptosis are highly linked physiological phenomena and some disease such as diabetes mellitus, cancer autoimmunity, Alzheimer's and Parkinson's and ischemia of brain and heart (Kannan and Jain 2000; Ryter et al 2007).

The mechanisms by which ROS/RNS cause or regulate apoptosis typically include receptor activation, caspase activation, Bcl-2 family proteins, and mitochondrial dysfunction (Ryter et al 2007).

1.5.6. Oxidative Stress and Autophagy

The tight interactions between oxidative stress and autophagygave in two aspects: the reduction of ROS byautophagy and the induction of autophagyby oxidative stress. Autophagy can contribute to decrease oxidative damages by engulfing and degradating oxidized substance. For example; ROS can induce the process of autophagy and, at the same time, are also controlled by autophagy. The consequences of those interactions between ROS and autophagy may have related with varied pathological conditions like ischemia/reperfusion (I/R), traumatic brain injury (TBI), tumor, and starvation. Autophagy contributes to clearing the cells of all irreversibly oxidized biomolecules (DNA, proteins and lipids), this is often all the additional reason why it may be included within the antioxidant and DNA damage repair systems (Filomeni et al 2014; Li et al 2015).

1.5.7. The Antioxidant Activities of TIGAR

TIGAR function that lowered fructose 2,6-bisphosphate levels during glucose metabolism in cells because TIGAR act as a fructose-2,6-bisphosphatase domain of Phosphofructokinase-2 or Fructose Bisphosphatase-2 (PFK-2 / FBPase-2) enzyme (Bensaad et al 2006). Additionally, FBPase-2 domain showed that the inhibition of PFK-1 resulted in the accumulation of fructose-6-phosphate; thereby the F6P is isomerized to glucose-6-phosphate. Finally, G6P is diverted into PPP. The PPP, which converts glucose-6-phosphate to ribose-5-phosphate for synthesis of nucleotides and NADPH to reduce DNA damage caused by ROS was reported to be activated in DNA damage response (Jackson and Bartek 2009; Yu et al 2015a). Regarding to these, TIGAR is requirement for NADPH produced by the PPP to generate GSH (key intracellular antioxidant) and decrease of antioxidant activates of ROS levels.

1.6. Aims and Objectives

This research aims to decipher the biological outcomes of the knockdown of TIGAR gene in A549 cell line utilizing the siRNA molecules followed by analysis of association between gene silencing of TIGAR and expression of certain markers linked with apoptosis (PCD-type-I) and autophagy (PCD-type-II).

2. MATERIALS AND METHODS

2.1. General

All chemical reagents were either of analytical or tissue culture grade, as appropriate for the experiment and were supplied some companies. A list of all the manufactures used for materials can be found in (Table 2.1) and for the kits can be found in (Table 2.2). A list of all the machines were used for the experiments can be found in (Table 2.3). Solutions for all practical work were prepared with ultra-pure water in a sterile condition (see table 2.4). Heat stable solutions and plastic ware (e.g. microcentrifuge tubes, pipette tips and other plastic wares) were sterilized by autoclaving at 121℃ (1 bar) for 15 min.

Table 2.1. All chemicals, reagents and materials were used in the experiments

Chemical, reagent and material	**Company name**	**Country of origin**
RPMI 1640 w/ L-Glutamine	Bio West	USA
Fetal bovine serum (FBS)	Gibco by life technology	USA
Penicillin-streptomycin	Gibco by life technology	USA
0.25% Trypsin EDTA	Gibco by life technology	USA
Tween-20	MERCK	Germany
Glycin	MERCK	Germany
Trichloroacetic acid (TCA)	MERCK	Germany
β-Mercaptoethanol	MERCK	Germany
NP-40	MERCK	Germany
EDTA	MERCK	Germany
EGTA	MERCK	Germany
β-glycerophosphate	MERCK	Germany
H_2O_2	MERCK	Germany

Table 2.1. (CONT.): All chemicals, reagents and materials were used in the experiments

NaOH	MERCK	Germany
Sodium dodecyl sulfate	MERCK	Germany
Phosphate buffer salt (PBS)	Sigma-Aldrich	USA
Bovine serum albumin (BSA)	Sigma-Aldrich	USA
Dimethyl sulfoxide (DMSO)	Sigma-Aldrich	USA
HCL	Sigma-Aldrich	USA
KCL	Sigma-Aldrich	USA
TEMED	Sigma-Aldrich	USA
Tris HCL	Sigma-Aldrich	USA
Tris (Trizma) base	Sigma-Aldrich	USA
Acetic acid	Sigma-Aldrich	USA
NaCl	Sigma-Aldrich	USA
Sodium deoxycholate	Sigma-Aldrich	USA
Na_3VO_4	Sigma-Aldrich	USA
NaF	Sigma-Aldrich	USA
Commasie Blue (G250)	Sigma-Aldrich	USA
NaN_3	Sigma-Aldrich	USA
2-thiobarbituric acid (TBA)	Sigma-Aldrich	USA
Malondialdehyde bis	Sigma-Aldrich	USA
Glycerol	Sigma-Aldrich	USA
Ethanol	Sigma-Aldrich	USA
Methanol	Sigma-Aldrich	USA
Trypan blue	Sigma-Aldrich	USA
Crystal violet dye	Sigma-Aldrich	USA
Ponceau S	Sigma-Aldrich	USA
H_3PO_4	Sigma-Aldrich	USA
Skim milk powder	Sigma-Aldrich	USA
P-Coumaric acid	Sigma-Aldrich	USA
PMSF	Sigma-Aldrich	USA
DTT	Sigma-Aldrich	USA
Benzamidine	Sigma-Aldrich	USA
Chloroform	Sigma-Aldrich	USA
Primers	Sentegen	Turkey
Antibodies	Santa Cruz Abcam	USA USA

Table 2.1. (CONT.): All chemicals, reagents and materials were used in the experiments

siRNA TIGAR	Santa Cruz	USA
Transfection medium	Santa Cruz	USA
Transfection reagent	Santa Cruz	USA
PVDF Membrane (0.45 µm)	Millipore	USA
X-ray film	Konica x ray film	USA
75 cm^2 T flask	Greiner	Germany
Cryotube	Greiner	Germany
5 and 10 ml serological pipettes	Greiner	Germany
15 and 50 ml centrifuge tubes	ISOLAB	Germany
0.2, 0.5 and 1.5 ml Eppendorf tubes	ISOLAB	Germany
6-well plates	Sigma-Aldrich	USA
96-well plates	Sigma-Aldrich	USA

Table 2.2. All kits were used for the experiments

Kits	**Company name**	**Country of origin**
RNA isolation kit [Quick-RNA™ MiniPrep]	Zymo research	USA
cDNA synthesis kit	Bioline	UK
Quantitative real-time PCR [2x qPCRBIO SyGreen Mix]	PCR Biosystems	UK
WST-1 cell proliferation and cytotoxicity assay Kit	Boster	USA
DCFDA - Cellular reactive oxygen species detection assay kit	Abcam	USA
NADPH assay kit (Colorimetric)	Abcam	USA

Table 2.3. All devices and equipment's were used in the experiments

Devices and equipment's name	**Company name**	**Country of origin**
Autoclave	Hirayama	Japan
Deep freeze	Nuaire	USA
Refrigerator	Arcelik	Turkey
Electrophoresis tank systems	Bio-Rad	USA
Incubator	Jeno Tech	Korea
CO_2 incubator	Nuaire	USA

Table 2.3. (CONT.): All devices and equipment's were used in the experiments

Light microscope	Olympus	USA
Spectrophotometer	Shimadzu	Japan
Laminar air flow cabinet	Esco	USA
Micropipette sets	Eppendorf	USA
Water bath	Nüve	Turkey
Magnetic mixer	Ika	Germany
Pure water device	Human	China
Quantitative real-time PCR Rotor-Gene Q	Qiagen	Germany
Thermal cycler	Sensoquest labcycler	Germany
Trans-blot system	Bio-Rad	USA
SpectraMax plus 384 microplate reader	Molecular Devices	USA
Sensitive balance	Denver Instrument	Germany
Spin vortex	Scientific Industries	USA
UV-Spectrophotometer	Shimadzu	Japan
X Ray film stabilization	Carestream	USA
pH meter	Thermo	USA
PCR thermal-cycler	SensoQuest	Germany
Shaker	Gerhardt	Germany
Ice machine	Hoshizaki	Japan
Table top centrifuge	Hermle	Germany
Fluorescence spectrometer	Perkin-Elmer Ls55	USA

Table 2.4. Solution names and their components were prepared for the experiments

Solution name	**Constituent of the solution**
RPMI complete medium - 1 L	Take 900 mL of RPMI medium 1640 complete media. Add 100 mL FBS and 10 mL penicillin (1000 IU/mL)-streptomycin (10 g/mL) solution. Mix them and then store at +4°C.
Freezing medium – 100 mL	Mix 10 mL DMSO with 90 mL FBS, then store at -20°C.

Table 2.4. (CONT.): Solution names and their components were prepared for the experiments

Bradford solution - 1 L	Weight 100 mg coommasie blue (G250). Dissolve at 50 mL ethanol, mix and wait 30 min. Then add 50 mL H_3PO_4 (85%) drop by drop. Add 100 mL ddH_2O and add 40 mL H_3PO_4 (85%) again. Fix to final volume till 1 L and then store at +4°C.
30% Acrylis bis solution - 1 L	Weight 292 g acrylamide and 8 g N, N'-methylenebisacrylamide. Dissolve in 100 mL ddH_2O by heating and mixing. Fix to final volume till 1 L then filtrated and then store at +4°C.
10 x PBS - 1 L	Weight 90 g NaCl, 11.45 g Na_2HPO_4, 2 g KCl, 2 g KH_2PO_4. Dissolve in about 0.5 L ddH_2O, adjust pH to 7.4. Fill up to 1 L and autoclave. Then store at room temperature.
10 x SDS Running buffer - 1 L	Weight 144.8 g glycine and 30.3 g tris base. Mix with 50 mL of 20% SDS solution-add this after dissolving the above two dissolve in about 0.5 L ddH_2O. Fill up to 1 L and store at room temperature (do not autoclave!).
10 x Western blot transfer buffer - 1 L	Weight 144.1 g glycine and 30.3 g tris base. Dissolve in about 0.5 L ddH_2O. Fill up to 1 L and store at +4°C (do not autoclave!).
1 x Western blot transfer buffer - 1 L	Mix 700 mL cold ddH_2O with 100 mL 10 x transfer buffer. Add 200 mL methanol, then use it.
10 x TBS - 1 L	Weight 87.66 g NaCl and 60.57 g tris base. Dissolve in 0.5 L ddH_2O and fill up to about 1 L. Add 37.5 mL of HCl and then adjust pH to 7.4. Autoclave it and store at room temperature.
1 M Tris-HCl (pH 7.4 to pH 8.0) - 1 L	Dissolve 121.1 g of tris base with 700 mL of ddH_2O by stirring. Add HCl in the following volumes to reach the desired pH: pH 7.4 = 70 mL of HCl; pH 7.6 = 60 mL of HCl; pH 8.0 = 42 mL of HCl. Fine adjust to the desired pH (7.4 - 8.0) with concentrated HCl. Add ddH_2O until final volume is 1 L. Autoclave to sterilize and store at room temperature.

Table 2.4. (CONT.): Solution names and their components were prepared for the experiments

1.5 M Tris-HCl pH 6.8 - 1 L	Dissolve 181.65 g of tris base with 700 mL of ddH_2O by stirring. Adjust the pH by adding the concentrated HCl. Begin by adding 118 mL and then fine adjust if needed. Add ddH_2O until final volume is 1 L. Autoclave to sterilize and store at room temperature.
20% SDS - 100 mL	Dissolve 20 g of SDS into 80 mL of ddH_2O by stirring. Add ddH_2O until final volume is 100 mL. Store at room temperature.
1% Bromophenol blue - 10 mL	Dissolve 100 mg of bromophenol blue with 10 mL of ddH_2O and mix. Store at room temperature.
1 x TBST - 500 mL	Add 50 mL of 10 x TBS to the 447.5 mL of ddH_2O. Add 2.5 mL of 20% Tween-20 and mix. Store at room temperature.
20% Tween-20 (Polysorbate 20) - 100 mL	Mix 20 mL of tween-20 with 80 mL of ddH_2O by stirring. Store at +4°C.
Coomassie stain - 1 L	Add 100 mL of glacial acetic acid to 500 mL of ddH_2O. Add 400 mL of methanol and mix. Add 1 g of Coomassie R250 dye and mix. Filter to remove particulates. Store at room temperature in a sealable container.
Fixing solution - 1 L	Mix 600 mL absolute ethanol with 75 mL glacial acetic acid. Bring up the volume to 1 L with ddH_2O. Store at room temperature.
5 x Laemmli buffer - 10 mL	Mix 2.5 mLof 20% SDS with 5 mL of glycerol. Add 0.01 g bromophenol blue. Then add 2.5 mL of 1 M tris-HCl, pH 6.8. Store in dark place at room temperature.
10% SDS - 1 L	Dissolve 100 g SDS in 1000 mL ddH_2O. Store at room temperature.
10% APS - 10 mL	Dissolve 1 g ammonium persulfate in 10 mL ddH_2O. Store at +4°C.
Blocking buffer - 10 mL	To 10 mL of T-TBS 1 x, add 0.5 g of non-fat dry milk or 0.5 g bovine serum albumin. Store at +4°C.
Stripping buffer - 1 L	Mix 10 mL β-mercaptoethanol with 200 mL SDS 10%. Add 137 mL tris-HCl 0.5 M, pH 6.8. Complete to 1 L with ddH_2O. Store at room temperature.
5 M NaCl - 1 L	Dissolve 292.3 g NaCl in 1000 mL ddH_2O. Store at +4°C.

Table 2.4. (CONT.): Solution names and their components were prepared for the experiments

10% NP-40 - 250 mL	Mix 25 mL NP-40 with 225 mL ddH_2O. Store at +4°C.
10% NaN3 - 100 mL	Dissolve 10 g NaN_3 in 100 mL ddH_2O. Store at +4°C.
10 N NaOH - 500 mL	Dissolve 200 g NaOH in 500 mL ddH_2O. Store at +4°C.
0.5 M EGTA (pH 8.0) - 100 mL	Dissolve 19.2 g EGTA in 100 mL ddH_2O. Adjust the pH by adding NaOH. Store at room temperature.
0.5 M EDTA (pH 8.0) - 1 L	Dissolve 146.12 g EGTA. 1000 mL ddH_2O. Adjust the pH by adding NaOH. Store at room temperature.
0.5 M NaF - 500 mL	Dissolve 10.5 g NaF in 500 mL ddH_2O. Store at room temperature.
250 mM Luminol - 25 mL	Dissolve 1.107 g luminol in 25 mL DMSO. Store at +4°C.
90 mM P-coumaric acid - 25 mL	Dissolve 0.37 g p-coumaric acid in 25 mL DMSO. Store at +4°C.
ECL solution 1 - 150 mL	Mix 15 mL tris-HCl (1 M, pH 8.5) with 135 mL ddH_2O. Add 1.5 mL luminal and 660 µL p-coumaric acid. Store at +4°C.
ECL solution 2- 150 mL	Mix 15 mL tris-HCl (1 M, pH 8.5) with 135 mL ddH_2O. Add 115 µL hydrogen peroxide (H_2O_2). Store at +4°C.
150 mM Standard lysis buffer - l L	Mix the following together: 20 mL 1 M tris-HCl (pH 8.0). 30 mL 5 M NaCl. 100 mL glycerol. 100 mL 10% NP-40. 10 mL 0.5 M EDTA (pH 8.0). 1 mL 0.5 M EGTA (pH 8.0). 100 mL 0.5 M NaF. 4.32 g 20 mM β-glycerophosphate. 5 mL 1 mM Na_3VO_4. Fix to final volume till 1 L of autoclaved ddH_2O then filtrated in to autoclaved bottle. Store at +4°C.

2.2. Thawing and Recovering Cell

Human A549 lung cancer cells were supplied by Bingol University Cancer Research Centre (BUCR). Vial was removed from the liquid nitrogen, immediately placed at 37°C water bath and stirred up vial continuously until the medium thawed approximately in 60 seconds. The top of the vial was wiped with 70% ethanol. Then, cell suspension was transferred to sterile 15 mL falcon tube that contain 5 mL pre-warmed complete growth RPMI 1640 medium, which contain 10% FBS and 1% Pen/Strep (10 unit/mL, 10 Mg/mL). The cell suspension was centrifuged 3 min at 1500 rpm at +4°C. Supernatant

was discarded, and then re-suspended cell gently with 3 mL fresh growth medium and transferred to 75-cm^2 with appropriate amount of medium. The cells were incubated in humidified incubator with supply 5% CO_2 at 37°C. After 24 h, cells were checked to ensure that the cells attached to the plate and the medium was changed every two days or when the color of indicator (phenol red) changed.

2.3. Cell Splitting and Maintenance

The cells were splitted after the confluences of cells reached to approximately 80% in the flask. The medium was removed by sterile serologic pipette inside the biosafety cabinet. Then, 3 mL PBS was added in to the flask and agitate the flask till the cover all the surface of the cells for removing the dead cells and washing the attached cells from remained medium which contain FBS. The PBS was removed by sterile pipette, to detach the cells, 0.25% Trypsin-EDTA added to cover the surface of attached cells, incubated for two to five min in 5% CO_2 humidified incubator at 37°C. The cells were checked under inverted microscope to observe if they detached completely. To deactivate the trypsin action, growth medium was added to the flask inside the biosafety cabinet, and then the cell suspension was mixed by sterile serologic pipette and collected within sterile 15 mL falcon tube, then centrifugation was done at 1500 rpm, +4°C for 3 min. Inside the cabinet, supernatant was removed and the cell pellet was resuspended with new pre-warmed fresh growth medium (RPMI) and they were poured into two new culture flasks. After that, the flasks were incubated in humidified incubator with 5% CO_2 at 37°C for 24 h. After 24 h, they were checked under inverted microscope to sure the cells attached and then the medium was changed one time in two days or when the changing of phenol red color. This process was continued until the confluence of cells reached 80%.

2.4. Transfection with Small Interfering RNAs (siRNA)

siRNA TIGAR kit, transfection medium, and transfection reagent were purchased from Santacruz biotechnology company. Untreated A549 cells, growing exponentially, were plated in 6-well plates at a density of 1×10^5 cells and allowed to attach overnight in a 5% CO_2 incubator set to 37°C. Once cells surpassed 50% confluency, transfection was performed according to the manufacturer's instructions. Briefly, the transfection mixture (30 nM siTIGAR RNA and 6 µL transfection reagent in each well) was diluted in 500 µL

transfection medium, gently mixed, and incubated for 30 min at room temperature. Next, the mixture was poured into the plate and incubated in a 5% CO_2 incubator at 37°C. After 6 h, 1 mL of complete RPMI medium was added to each well without discarding the transfection mixture. 24 h after transfection, cells were trypsinized in 0.25% Trypsin-EDTA, re-suspended in fresh media, and re-plated for cell viability and ROS, NADPH, and clonogenic cell survival assays. The harvested cells were also used for western blotting and qRT-PCR assays.

2.5. Measurement of Cell Viability

The short-term effects of TIGAR silencing on tumor cell growth were assessed using a WST-1 assay kit. For siRNA transfection, as described in previous section, 5,000 of transfected cells were cultured in each well of 96-well plates in 100 µL growth medium. After 24 h of incubation, 10 µL of WST-1 was added to each well and incubated for 4 h, after which a WST-1 assay was performed. The percentage of growth inhibition was calculated as (OD vehicle-OD treatment), where ODs were measured using a SpectraMax plus 384 microplate reader at 420 and 480 nm, respectively (Molecular Devices LLC, USA).

2.6. Clonogenic Survival Assay

The long-term effects of TIGAR silencing on tumor cell proliferation were analyzed using a colony-formation assay. 24 h after siRNA transfection, 1×10^2 A549 cells were plated in triplicate in 6-well plates. The media was changed every 3 days for 12 days, then discarded; cells were washed once by PBS, then fixed by adding methanol: acetic acid (3:1) and incubated for 5 min, after which the fixing solution was removed. Staining was performed using 0.5% crystal violet in methanol for 15 min; cells were then gently washed with distilled water and left to dry at room temperature. During microscopic observation of cells, colonies consisting of 50 cells were counted as single colonies (Chen et al 2015).

2.7. Total Cellular ROS Levels

The ROS effects of TIGAR knockdown on tumor cell growth were assessed using a DCFDA assay kit. In 96-well plates, transfected cells were cultured (25,000 per well) in

200 µL growth medium and incubated for 24 h at 37°C in a 5% CO_2 incubator. Following incubation, the medium was discarded for each well and washed with 100 µL of 1 × buffer; 100 µL DCFDA was then added to each well, followed by 45 min of incubation at 37°C in dark conditions (5% CO_2 incubator). DCFDA was then discarded and 100 µL of 1× buffer added, after which the plate was measured using a fluorescence spectrometer plate reader at Ex/Em=485/535 nm using the end point mode (Perkin-Elmer LS-55, USA).

2.8. Measurement of NADPH Levels

The effects of TIGAR silencing on tumor cell growth was assessed using an NADPH assay kit to determine NADPH levels. In 96-well plates holding 10,000 of transfected cells per well, cells were cultured in 100 µL growth medium. Cell lysate was then extracted by lysis buffer (provided by kit), 50 µL of which was added to each well for each sample. After adding 50 µL of reaction mixture to each well, an NADPH assay was performed. NADPH percentage levels were calculated as (OD vehicle-OD treatment), where ODs were measured using a SpectraMax plus 384 microplate reader at (460 nm).

2.9. Protein Extraction and Western Blot Analysis

2.9.1. Cell Lysate

After approximately 80-90% of their confluency, the medium of cells from each well of well plate was aspirated by aspiration, then washed by PBS and then aspirated again. Cells were trypsinized by adding enough trypsin-EDTA for 5 min and then added growth medium to deactivate trypsin activation, after that cells suspension were collected in the falcon tube and then centrifuged at 4000 rpm / $+4^{o}$C for 5 min, then discarded supernatant. Finally enough protein lysate (Standard lysis buffer) was added and left at room temperature for 30 min. Protein lysate was extracted from cells using a lysis buffer. After 30 min, the lysates were centrifuged at speed 14000 rpm for 30 min and then the supernatants were collected, the pellets were discarded, and the lysates preserved at -20°C.

2.9.2. Bradford Protein Assay

To determine the total protein concentration of a sample, the Bradford protein assay is a method most routinely used. Protein concentrations were determined manually using Bradford solution. The principle of detection is a binding of the Coomassie blue dye with the proteins in a sample. The more protein is present, the more Coomassie dye binds to them. This assay is colorimetric; the color of the examined samples will turn from brown to blue as the protein concentration increases and vice versa. Absorbance is measured at a specific wavelength which is 595 nm.

Bovine serum albumin (BSA) was used as a protein standard, the initial concentration of which was 2000 µg/mL. It was serial diluted in deionized water by using the Eppendorf tubes at concentrations of 1000, 750, 500, 250, 125, 50 and 25 µg/mL. Upon preparation using ultra-pure water, standards were mixed by vortex machine to ensure solutions are homogeneous and 10 µL of each was added in triplicate into the Eppendorf tube (triplicates were used to obtain more accurate results). Also, 10 µL of deionized water were used as a control sample. Then, a 1.5 mL of Bradford solution was added to each one of them. They were briefly shaken just before absorbance of all samples by shaker, and then they were measured by using UV-1800 spectrophotometer at 595 nm. The absorbance readings obtained were used to obtain a standard curve, so the protein concentration of the samples were determined by comparison to that series standard protein concentration in linear curve, and finally extrapolation is used to determine their concentrations (Ernst and Zor 2010).

2.9.3. Sample Preparation for Loading

Cell lysates were mixed with Laemmi buffer (5×) as in 5:1 ratio. Sample buffer contains Coomassie blue, allowing visualization of the protein bands and contains SDS also, which denature protein’s disulphide bonds and make them negatively charged. These were then mixed well by vortex machine and samples collected by a brief spin on a micro-centrifuge in tube. Samples were then boiled at 95°C in a heat-block for 5 min (this denatured the proteins, to make sure that the proteins do not have a secondary, tertiary or quaternary structure). Finally, following quick mixing by vortex machine, samples were by brief centrifugation (as above).

2.9.4. SDS-PAGE

SDS-PAGE is an abbreviation for Sodium Dodecyl Sulphate Poly Acrylamide Gel Electrophoresis. It is a technique for separating proteins based on their polypeptide length chains or on their molecular weights; proteins have ability to move within an electrical current because of an overall negative charge. This is achieved by adding SDS detergent to allow protein migration and to maintain their polypeptide chains. Protein structures are coated by SDS and move proportionally to their molecular weight, i.e. small molecular weight migrates through SDS quicker than high molecular weights because of their sizes, after applying electrical charges across all proteins in the sample (Sambrook et al 1989)12% SDS-PAGE gel was prepared by the Bio-Rad mini protean system. Tris/glycine sodium dodecyl sulfate polyacrylamide gel electrophoresis 12% was used for this work (see table 2.5). The gel was prepared within 30 min. Then, the comb was gently removed and then rinsed with deionized water. The cassette was placed and fixed on the tank of the Bio-Rad system; the false cassette was then added. After this, 200 mL of fresh running was added to the inner chamber and also 600 mL to the outer chamber. 5 µL of a set of protein molecular weight standards (Denoted marker) was loaded into first well of the gel by using a gel tip. Following this, 20 µL of each sample was added to the other wells, and the location of each sample loaded was noted to ensure it was clear which well corresponded to which protein lysate (and the amounts loaded). The lid of the system was put in place, the positive and negative electrodes were connected to a power pack and the electrophoresis was performed. The gel was running by giving electricity 20 mA for 30 min at first, raised the electricity to 40 mA by using power supply (Bio-Rad, USA) until loaded protein reached the last destination of a polyacrylamide gel.

Table 2.5. Solutions were used for tris/glycine sds-polyacrylamide gel electrophoresis

Reagents	**Resolving gel (5 mL)**	**Stacking gel (2 mL)**
Deionized water	1.7 mL	1.4 mL
30% acrylamide: bis-acrylamide	2 mL	330 µL
1.5 M Tris-HCl, pH 8.8	1.3 mL	….
1 M Tris-HCl, pH 6.8	….	250 µL

Table 2.5. (CONT.): Solutions were used for tris/glycine sds-polyacrylamide gel electrophoresis

10% SDS	50 µL	20 µL
10% APS (catalyst)	50 µL	20 µL
TEMED (catalyst)	2 µL	2 µL

2.9.5. Immunoblotting (Western Blot)

The western blot is an analytical procedure used to select specific proteins in a sample. This technique uses the gel electrophoresis to resolve denatured or native proteins by their sizes of the polypeptides or by the 3-D structure of the proteins, followed by protein detection using antigen-specific antibodies. In this project, proteins were separated by SDS-PAGE electrophoresis. The protein bands were transferred onto a membrane to allow visualization and analysis, by the addition of primary antibodies that were specifically for those protein bands; secondary antibodies were used to visualize primary antibody binding. Resolved proteins were transferred to a strong, competent PVDF membrane (Polyvinylidene Fluoride). The western blot technique is based on the fact that cellular proteins will strongly bind to PVDF (and nitrocellulose membranes), and the membranes are used to subsequently detect proteins of interest such as (TIGAR, Caspase-3, Beclin-1, LC 3 I and II, NFκB, HO-1 and GAPDH.

2.9.6. Blotting Procedure

The process followed is a modification of the manufacturer's recommendations (Bio-Rad). After running gel, in preparation for blotting, the blotting pads and filter papers cut to the same size of the gel were all soaked in transfer buffer. This was done gently by using tweezers because the integrity of the filter papers was lost when it is wet. The PVDF membrane was also cut to the same size and soaked for 30 seconds in methanol and subsequently rinsed in distilled water. The gel cassette was then gently removed and excess gel was removed as well using a gel knife. A piece of filter paper was placed on top of the gel, and then gently removed from the cassette and placed onto the blotting pads on the contrary. A transfer membrane was placed on the gel followed by another piece of filter paper. To avoid any air bubble, gentle rolling was done and then other blotting pads were put (see figure 2.1). The western blot apparatus was placed in the Bio-

Rad system. The inner and outer chamber was filled with transfer buffer until 2 cm from the top. The device system was kept in a box of ice to make sure it did not overheat. Then, it was connected to the power supply and run at180 mA for 2 h. Once complete the device was disconnected and opened. The transfer membrane was gently placed into a square petri dish containing TBS. The membrane stained with a reversible stain like Ponceau stain to be sure there were the protein bands on the membrane and there was not any air bubble during protein transformation. In all movement, tweezers were used instead of fingers (this might create 'noise' on the blot).

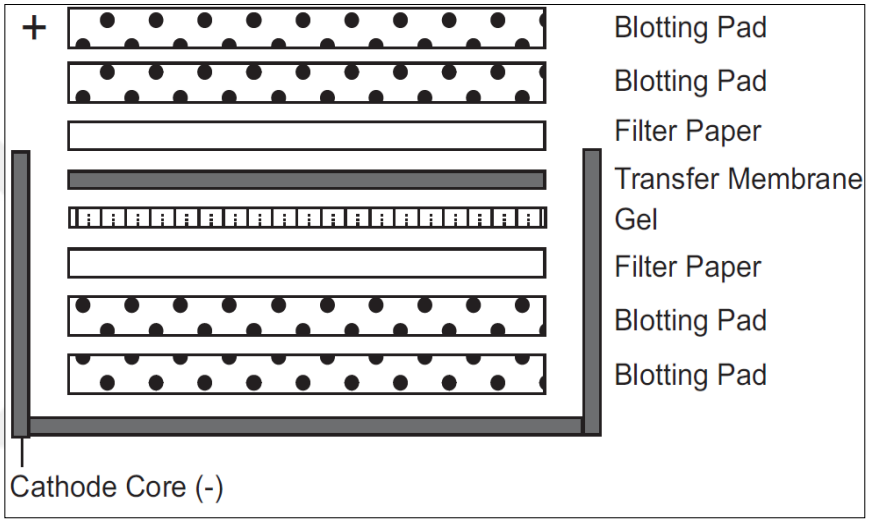

Figure 2.1. Making western blotting by Bio-Rad System. A diagram shows how the gel, transfer membrane, filter papers and blotting pads are used for blotting as a single sandwich during a typical western blotting experiment

2.9.7. Blocking the Membrane

For western blotting, primary and secondary antibodies are used to visualize the target protein bands. However, antibodies may bind to the membrane in a non-specific fashion. To reduce this problem, membranes had to be blocked to avoid non-specific antibody interactions.

Once the transfer process (blotting) was completed, the PVDF membrane was removed and placed directly in TBS in a square-shape Petri dish to wash any excess of solution from the blotting procedure. The TBS was removed and the membrane incubated with 10 mL of blocking buffer 5% BSA in TBST. The membrane was soaked in the blocking

buffer for 1 h with gentle shaking on a rock shaker at room temperature. After that, the blocking buffer was removed and the membrane was washed briefly using the TBST.

2.9.8. Membrane Labeling

Protein detection on membranes is performed using antibody-mediated labeling. For detecting the effect of siRNA-Tigar on apoptosis, autophagy and oxidative stress pathway in A549 cells, some protein markers were analyzed by the different primary antibodies in different dilution factor. Antibodies were diluted within 5% BSA solution, according to the manufacturers' recommendations, then incubated PVDF membrane overnight with primary antibodies (see table 2.6) solution with gentle agitation. After primary antibody, the membranes washed 5 times with TBS-T solution for 5 min except first time were 10 min, and then incubated 1 hr with secondary antibody (see table 2.7) diluted in 5% BSA solution. Membranes washed 5 times with TBS-T solution for 5 min, first time were 10 min.

Table 2.6. The primary and secondary antibodies were used for detection in immunoblotting that used for detecting the amount of desired protein inside the cells. It contains the primary antibodies names, concentrations and the companies of origin

Name of antibody	Dilution	Obtained from	Secondary antibody
Anti Tigar	1:500	Santacruz biotechnology	Anti-mouse
Anti Caspase-3			Anti-rabbit
Anti Beclin-1			Anti-mouse
Anti Lc3a			Anti-rabbit
Anti GAPDH			Anti-mouse
Anti NF-κB P65	1:2000	Abcam	Anti-rabbit
Anti Heme Oxygenase-1	1:2000	Abcam	Anti-rabbit

Table 2.7. The secondary antibodies were used in Immunoblotting assay

Name of antibody	Dilution	Obtained from
Anti-mouse	1:5000	Santacruz biotechnology
Anti-rabbit		Abcam

2.9.9. Detection

The PVDF membrane incubated with ECL solutions (solution 1 and 2) for 2 min, and then the membrane placed on the film-developing system with x-ray film (Konica, USA) in dark place side by side by using cassette, exposure times were 3 seconds to 5 min according to different types of antibodies, and then washed film by developer and fixer solutions inside x-ray machine (Carestream, USA). Finally, the bands analyzed by scanning the film and using (Adobe Photoshop CS5) software to check their densitometry levels (Mahmood and Yang 2012).

2.10. RNA Extraction and qRT-PCR

2.10.1. Total RNA Isolation

Total RNAs from cells were extracted using (Quick-RNA™ MiniPrep) kit. The cells were transfected as described in section 2.4. Then, they were trypsinized and centrifuged to have a cell pellet, after that they washed once by cold PBS and centrifuged again, then added 300 µL RNA lysis buffer (provided by the kit), followed by centrifugation at 14000 rpm for 1 mint. The supernatant was transferred into a (Spin-Away™ Filter - yellow one in the kit) in a collection tube and centrifuged at 14000 for 1 minute to remove the majority of gDNA, and then the flow-through was saved. Ethanol (95-100%) was added to the sample in a ratio (1:1). Then, mixed well and the mixture was transferred to a (Zymo-Spin™ IIICG Column1 - green one in the kit) in a collection tube and centrifuged for 30 seconds. The flow-through was discarded. To remove trace DNA removal, the column was washed with 400 µL RNA wash buffer. Then, centrifuged for 30 seconds and the flow-through was discarded. For each sample to be treated, 80 µL (DNase I Reaction) was added directly to the column matrix and incubated at room temperature (20-30ºC) for 15 min, then centrifuged for 30 seconds. After that, 400 µL (RNA Prep Buffer) was added to the column and centrifuged for 30 seconds. The flow-through was discarded and 700 µL (RNA Wash Buffer) was added to the column and centrifuged for 30 seconds. The flow-through was discarded and 400 µL (RNA Wash Buffer) was added again and centrifuged the column for 2 min to ensure complete removal of the wash buffer. Finally, the column was carefully transferred into an (RNase-free) tube and 100 µL (DNase/RNase-Free Water) was added directly to the column

matrix and centrifuged for 30 seconds to get elute RNA. The eluted RNA was checked, by SpectraMax plus 384 microplate reader, for quality to know if there is any contamination in the sample. The A260/A280 ratio is an indication of the level of protein contamination in the sample. Our sample values were between 1.8-2.0 and considered acceptable. The 260/230 ratio is an indication of the level of guanidine salts and phenol contamination in the sample.

2.10.2. cDNA Synthesis

cDNA synthesis was performed from 1 µg of RNA using a cDNA synthesis kit (Bioline, UK); a thermal cycler (Sensoquest labcycler, Germany) machine was used. The mastermix was prepared on ice and mix gently by pipetting. 4 µL (TransAmp Buffer-5x) was mixed with 1 µg of isolated RNA, then 1 µL (Reverse Transcriptase) was added to the mixture. Finally, the volume was fixed till 20 µL by adding (DNase/RNase free-water). The sample was put in to the thermal cycler and the program was set up: [25°C for 10 min for primer annealing, 42°C for 15 min for reverse transcription, 85°C for 5 min for inactivation step, and finally +4°C to hold the sample till use it].

2.10.3. Real Time PCR

Real-time PCR amplification was performed by using (2× qPCRBIO SyGreen Mix) kit (PCR Biosystems, UK) and using a Rotor Gene PCR system (Qiagen, Germany). Real-time RT-PCR mastermix was prepared like the following: [10 µL of 2x qPCRBIO SyGreen Mix, 0.8 µL forward primer 10 µM, 0.8 µL reverse primer 10 uM, 4 µL cDNA template, and finally fixed the total volume till 20 µL by PCR grade dH_2O]. The PCR components were mixed briefly and placed the tube into the real-time cycler. The real-time cycler was set up according to the following table (Table 2.8), depending on the real-time cycler and running the program that were used. Expression mRNA was quantified by using a primer. The primers were purchased from (Sentegen Company-Turkey) and their sequences were designed previously via NCBI website (see table 2.9). The CT (threshold cycle) value of TIGAR and others amplification were normalized to that of the GAPDH control. Gene expression was quantified relative to the housekeeping gene GAPDH according to the comparative ΔΔCt, Livak method (Livak and Schmittgen 2001).

Table 2.8. The real-time cycler was set up according to the manufacture's instruction

Cycles	Temp.	Time	Notes
1	45°C	10 min	Reverse transcription
1	95°C	2 min	Polymerase activation
40	95°C	5 seconds	Denaturation
	60°C	10 seconds	Annealing
	72°C	5 seconds	Extension (acquire at end of step)

Table 2.9. It shows the sequences of primers and their accession numbers. These websites were used for design the primers and check for their specify {https://www.ncbi.nlm.nih.gov/nuccore, http://bioinfo.ut.ee/primer3-0.4.0/primer3/}

No.	Name of Genes	Primer Sequence (20)Base pair per each	GenBank Accession No.
1	CASP 3 (Capsase-3)	Forward: ATTGTGGAATTGATGCGTGA Reverse: GGCAGGCCTGAATAATGAAA	NM_004346
2	BECN1 (Beclin-1)	Forward: TCACCATCCAGGAACTCACA Reverse: TTCAGTCTTCGGCTGAGGTT	NM_001313998
3	MAP1-LC3A (LC3 I and II)	Forward: TCAACATGAGCGAGTTGGTC Reverse: AAGCCGTCCTCGTCTTTCTC	NM_032514
4	C12ORF5 (TIGAR)	Forward: CGGCATGGAGAAACAAGATT Reverse: CATGGTCTGCTTTGTCCTCA	NM_020375
5	GAPDH (GAPDH)	Forward: CCACCCAGAAGACTGTGGAT Reverse: TTCTAGACGGCAGGTCAGGT	NM_001256799
6	NFκB1 (NFκB)	Forward: CCTGGATGACTCTTGGGAAA Reverse: TCAGCCAGCTGTTTCATGTC	NM_001165412
7	HMOX1 (HO-1)	Forward: ATGACACCAAGGACCAGAGC Reverse: GTGTAAGGACCCATCGGAGA	NM_002133

2.11. Statistical Analysis

All data were expressed as means ± standard deviation. Statistical testing was performed using the GraphPad Prism 5.01 software statistical package (GraphPad Software). A paired t-test was used for comparing the two groups. Significant differences at $p< 0.05$, 0.01 and 0.001 are indicated by *, **, and ***, respectively.

3. RESULTS

3.1. siRNA and BPA

In order to study in the lung cancer, A549 cell line was used. The cells were seeded and prepared as described in the materials and methods sections 2.2 and 2.3. To silence the TIGAR protein in the A549 cell line, siRNA assay was performed. Transfection with small interfering was performed as described in section 2.4. As shown in figure 3.1, the cells morphology was examined under light microscope to check the rate of healthy with adherent cells inside of the plate and wells. As expected, the rates of attached cells were decreased after transfection the cells with siRNA (see figure 3.1.A), this is compared with control cells that were not transfected with siRNA (see figure 3.1.B). The cells look more shrinkage rather that oval shape, and the cell death markers that increased after knockdown TIGAR, so the viability of the cells were decreased. The analysis about cell viability will be discussed in the next section.

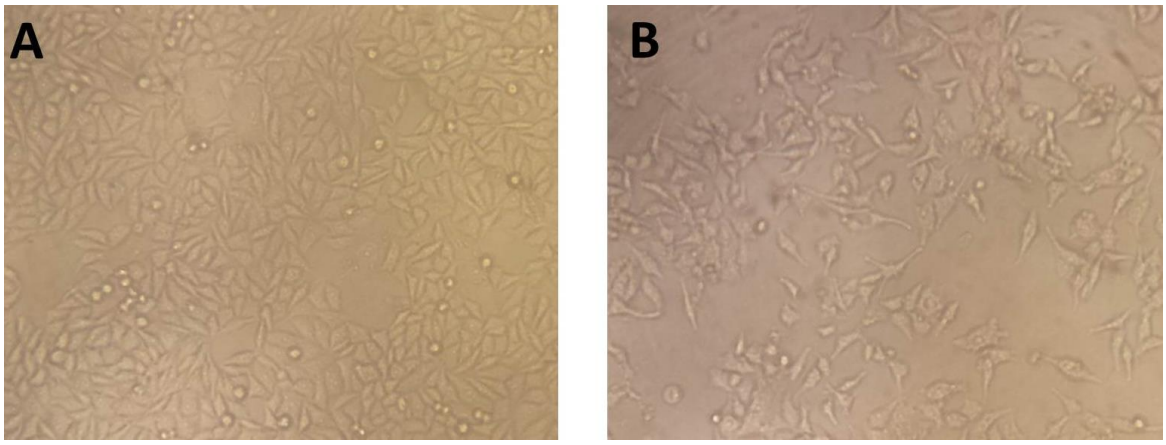

Figure 3.1. It shows the A549 cells under microscope 40×. (A) A549 cells before transfection, 24 h after seeding with siTIGAR. (B) A549 cells after transfection, 24 h after seeding

Following transfection, the samples were assayed by western blot. For this reason, the lysates were checked their concentration by Bradford Protein Assay. As explained in the section 2.9.2. The lysate analyzed by taking absorbance and read their measurements at 595nm by the spectrophotometer. Figure 3.2 is a composite image of excel software that collected all absorbance data, subtracted background, produced average readings. Moreover, the excel software produced a calibration curve based on the protein standards (serial dilutions), which allowed quantification of the lysate samples concentrations on the basis of the calibration (standard) curve.

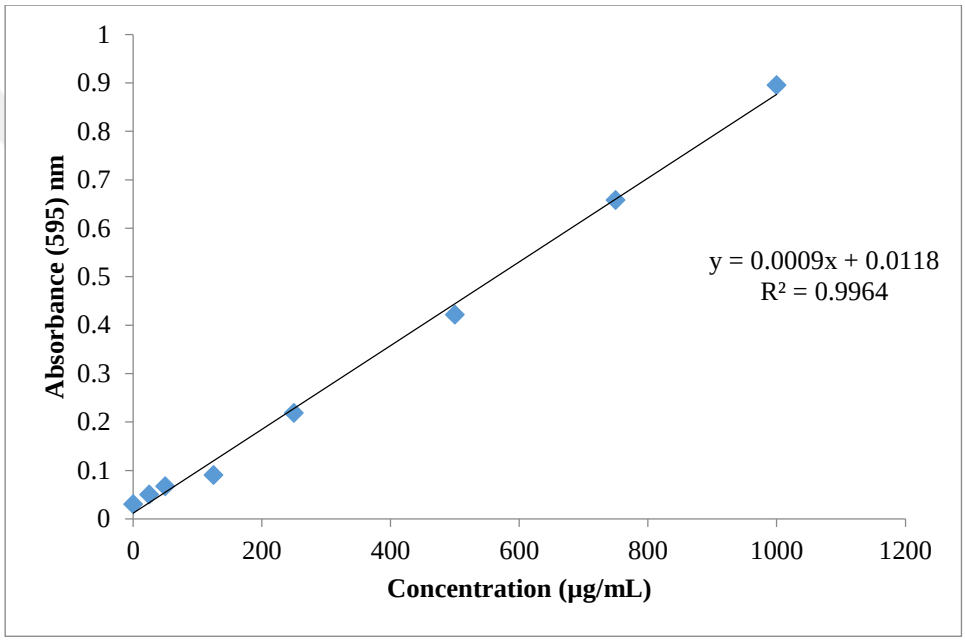

Figure 3.2. Protein standard assay curve showing the absorbency of the Bovine serum albumin standards, which the unknown proteins (lysates) concentrations can be extrapolated from the standard curve. R^2 value = 0.99

3.2. TIGAR-siRNA Down-Regulates TIGAR Expression in A549 Cells

TIGAR was the first protein that was evaluated by western blot in our experiments. Lysate of 25 µg from A549 cells were loaded into a gel, separated by SDS and then analyzed by western blotting; these procedures were described in section 2.9. The protein bands were labeled by using primary and secondary antibodies as mentioned in section 2.9.8. Figure 3.3.B illustrates the results of the GAPDH and TIGAR by western blot. Labeling was carried out on the same membrane to ensure the validity of the TIGAR

result by confirming correct loading. The molecular ladder weight marker was used. The membrane was visualized by ECL solution.

Before the presence of TIGAR, GAPDH protein was detected, it was essential to first carry out a western blot for this protein because GAPDH is a housekeeping protein presents in most the cell lines. Detecting this protein generated visual bands as proof that all loading and antibody tagging were efficient and reliable, so the results later derived by the TIGAR in western blot would be reliable and true. GAPDH has a predicted molecular weight of 37 kda, as clearly shown by the bands in the figure 3.3. The size of the bands increases when the amounts of the lysate increase, clearly shown by the bands in the figure 3.3. The analysis TIGAR knockdown will be discussed in the discussion section.

The mRNA level of GAPDH and TIGAR were also evaluated by qRT-PCR. As describes in section 2.10, the total RNA for both control and transfected cells were isolated. The eluted RNA was checked, by SpectraMax plus 384 microplate reader, for quality and to know if there is any contamination in the sample. Then, cDNA was synthesized from 1 µg of RNA using a cDNA synthesis kit. Finally, real-time PCR amplification was performed by using kit and primers for GAPDH and TIGAR.

Previous studies have reported that siRNA TIGAR down-regulated TIGAR expression in glioblastoma cells, hepatocellular carcinoma, and prostate cancer (Huang et al 2017; Tai et al 2016; Wanka et al 2012; Xie et al 2014; Yu et al 2015a). As expected, TIGAR expression levels were markedly down-regulated in the A549 cell line; we checked the expression status of TIGAR mRNA and protein by using a qRT-PCR and western blot analysis, respectively, after normalization by the housekeeping protein GAPDH. RNAi was performed by transient transfecting siRNA to silence TIGAR expression in A549 cells. Western blotting was used to measure TIGAR expression. We treated A549 cells with a three target-specific of siRNAs targeting TIGAR (Santa cruz biotechnology kit). Based on western blot data from the 24 h treatment sample, siRNAs reduced TIGAR expression by approximately 55% relative to control cells (Figure 3.3.B). Next, we examined inhibition of TIGAR mRNA by performing a qRT PCR on samples from 24 h after transfection. Similar to the western blot, the qRT PCR result as in (Figure 3.3.A) also demonstrated that siRNA had interference efficiency (nearly 50%) of down regulation of the TIGAR relative to the control cells.

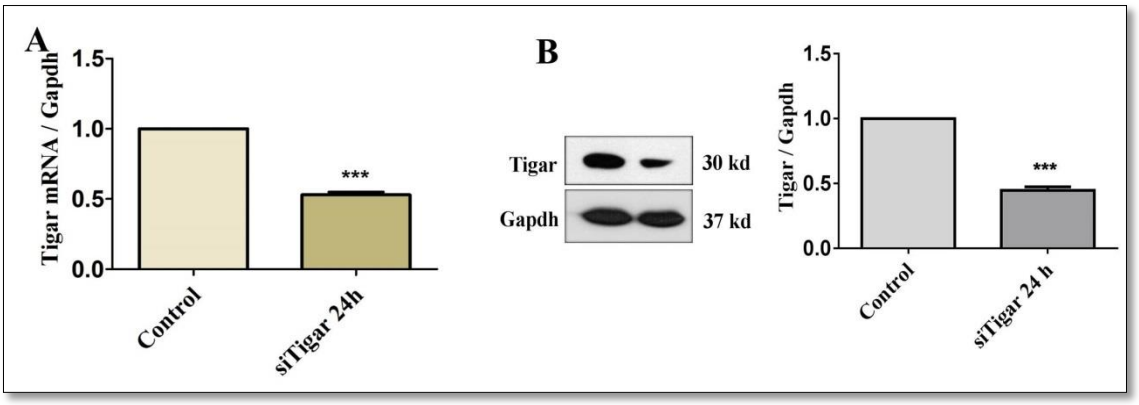

Figure 3.3. siRNA TIGAR knockdown in A549 cells. Transfection of siRNAs was performed to knockdown TIGAR expression for 24 h. Expression of TIGAR was detected using western blotting and qRT PCR. For loading control, GAPDH, a housekeeping protein was used. Protein band intensity analysis was performed with Image J software and graphs were plotted using GraphPad Prism 5.01 software. (A) Expression of TIGAR mRNA levels was down regulated compared with its level in the control-A549 cell line without transfection by siTIGAR. (**B**) Expression of TIGAR protein level was down regulated compared with its level in the control-A549 cell line without transfection by siTIGAR. Data were expressed as mean ± SD with three independent experiments. (* $p< 0.05$ vs cont., ** $p<0.01$ vs cont. and *** $p<0.001$ vs cont.)

3.3. TIGAR Knockdown Affects A549 Growth Rate and Colony Formation

In the first and second experiments, A549 cells were transfected by siRNA TIGAR, then assayed by cell viability and clonogenic assays; these procedures were described in sections 2.5and 2.6. In the first experiment, growth rate of TIGAR-silenced cells was monitored of WST-1 kit. It had a yellow color that was reduced to formazan dye as a purple color by some enzymatic activities from the cells during their growths, and then was quantified, such enzyme like NAD(P)H-dependent cellular oxido reductase enzymes. The percentage of growth inhibition was calculated as (OD vehicle-OD treatment), where ODs were measured using a SpectraMax plus 384 microplate reader at 420 and 480 nm, respectively. The second experiment was to check the cell survival based on the ability of a single cell to grow into a colony. The colony is defined to consist of at least 50 cells. After two weeks past of seeding, the cells were fixed by methanol: acetic acid (3:1) to avoid detaching the cells from the plates. Then, the cells were stained by crystal violet to visualize the colonies by naked eye.

In accordance with the scope of this study, we aimed to explore the biological consequences of specific silencing of TIGAR in the A549 cell line. We evaluated both short- and long-term cell viability via clonogenic assay and cell proliferation assay,

respectively. We investigated TIGAR inhibition by siRNA and the results showed the inhibition both cell growth and colony formation in A549 cells. A WST-I assay indicated that treating A549 cells using siTIGAR inhibited cell viability. Reduced A549 cell viability was strongly related to silencing of TIGAR following siTIGAR treatment. After TIGAR was down-regulated by RNAi for 24 h, cell viability decreased noticeably compared to an untreated control (Figure 3.4.A). A549 TIGAR-silenced cells also showed a clear reduction of colony formation when compared to control cells (Figure 3.4.B).

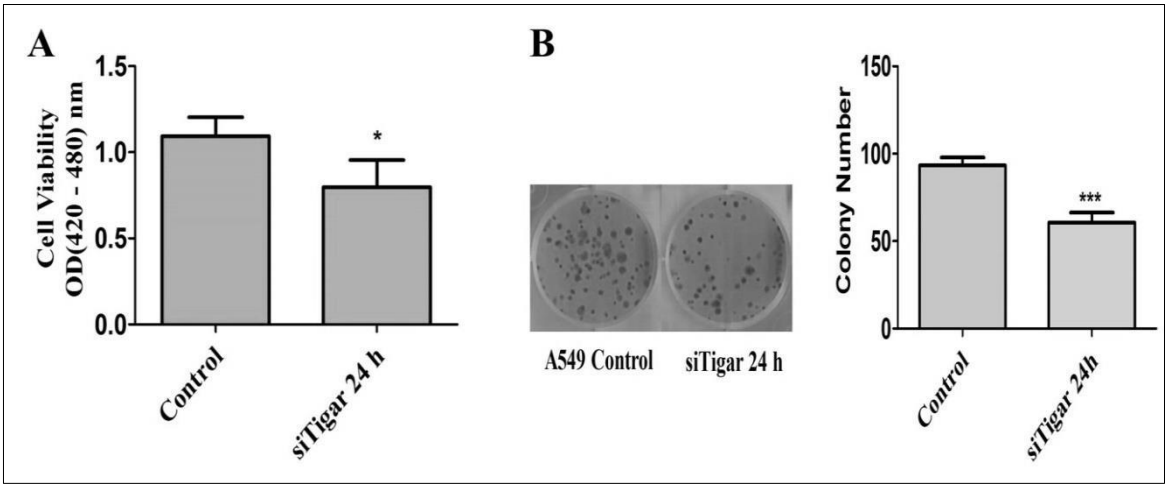

Figure 3.4. siRNA TIGAR knockdown inhibited cell viability and colony formation of A549 cells. Transfection of siRNAs was performed to knockdown TIGAR expression for 24 h. The graphs were plotted using GraphPad Prism 5.01 software. (A) Short-term effects of cell growth were assayed by WST-1 assay, which shows that nearly 28 % of cell viability decreased compared to a control from the A549 cell line without transfection by siTIGAR. (B) Long-term effects of cell growth were assayed by a colony formation assay, which shows the colony decreased by nearly 35% compared with colony formation in a control from the A549 cell line without transfection by siTIGAR. Data were expressed as mean ± SD with three independent experiments. (* $p< 0.05$ vs cont., ** $p<0.01$ vs cont. and *** $p<0.001$ vs cont.)

3.4. TIGAR Knockdown Induces an Decreasing NADPH Level via ROS

In the third and fourth experiments, A549 cells were transfected by siRNA TIGAR, then assayed by ROS and NADPH assays; these procedures were described in sections 2.7 and 2.8. In these experiments ROS and NADPH levels in silenced cells were monitored by DCFDA and NADPH colorimetric assay kits respectively.

The redox state was evaluated by assaying total ROS and NADPH levels. TIGAR is reported to inhibit glycolysis, subsequently increasing NADPH levels and decreasing

intracellular ROS levels, and thus protecting the cells from intracellular ROS associated with apoptosis. To determine whether silencing TIGAR was associated with increased ROS levels, we measured ROS levels in cells transfected with TIGAR siRNA. Results indicated that ROS levels were slightly increased in A549 cells after TIGAR knockdown (Figure 3.5.A). Also, NADPH levels were evaluated to determine whether decreasing viability and increasing cell death induced by silencing TIGAR was related to NADPH levels, we checked the NADPH levels in the cells transfected with TIGAR siRNA. Results showed that NADPH levels decreased slightly in A549 cells after TIGAR knockdown (Figure 3.5.B). Down regulation of NADPH and upregulation of ROS levels coincided with a decrease in TIGAR protein and increased cell deaths in other associated proteins as a consequence of TIGAR knockdown.

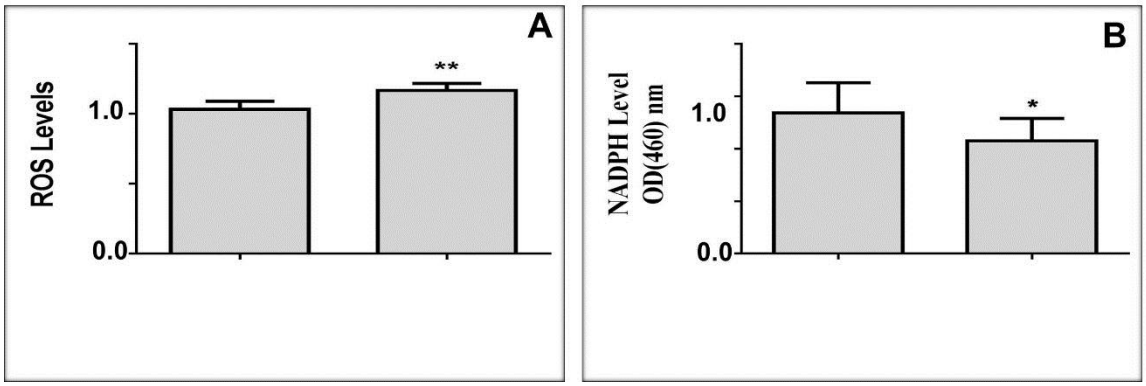

Figure 3.5. siRNA TIGAR knockdown enhances an increasing ROS and decreasing NADPH levels. Transfection of siRNAs was performed to knockdown TIGAR expression for 24 h. Graphs were plotted using GraphPad Prism 5.01 software. (A) ROS levels were detected by DCFDA assay, and were shown to have increased by nearly 12% compared to ROS levels in the control-A549 cell line without transfection by siTIGAR. (B) NADPH levels were detected, showing that NADPH levels decreased by nearly 20% compared to NADPH level in the control-A549 cell line without transfection by siTIGAR. Data were expressed as mean ± SD with three independent experiments. (* p< 0.05 vs cont., ** p<0.01 vs cont. and *** p<0.001 vs cont.)

3.5. TIGAR-Specific siRNA up-Regulates Apoptosis Markers

Following detection of TIGAR the next protein of interest was Caspase-3, as apoptotic marker. This experiment was done by the same procedures as mentioned earlier. Lysates were loaded at 25 µg per well for control and sample into a new gel, separated by SDS and then analyzed by western blotting; these procedures were described in section 2.9. The protein bands were labeled by using primary and secondary antibodies as mentioned in section 2.9.8. Figure 3.6. illustrates the results of the GAPDH and Caspase-3 by

western blot. They produced on the same membrane to confirm the validity of the result of Caspase-3 expression by ensuring accuracy when loading could be determined and visualized. The molecular ladder weight marker was used. The membrane was visualized by ECL solution. Before the presence of Caspase-3, GAPDH protein as housekeeping protein was detected by the same procedures as mentioned earlier (see figure 3.6). The primary antibody was used for Caspase-3 that has a predicted molecular weight of 35 kda, clearly shown by the bands in the figure 3.6. The analysis of Caspase-3 will be discussed in the discussion section. The mRNA level of GAPDH and Caspase-3 were also evaluated by qRT-PCR by the same procedures as mentioned earlier. To identify apoptotic cell death mechanism in A549 cells occurred in TIGAR-silenced cells, we first observed silencing of TIGAR expression by siRNA, which can activate cell death signaling in A549 cells. Then, the cells were used in both western blots and qRT PCR assays to check the levels of Caspase-3 as apoptotic marker. Caspase-3 as a cell death marker was indicated in the transfected and control A549 cells, which was triggered by the silencing of TIGAR expression by RNAi. Results indicated that cell growth was inhibited, with evidence of apoptotic cell death after TIGAR silencing in A549 cells. Results showed that the mRNA and protein expression levels of apoptotic marker, Caspase-3, had significantly increased after silencing of TIGAR (Figure 3.6.A and B).

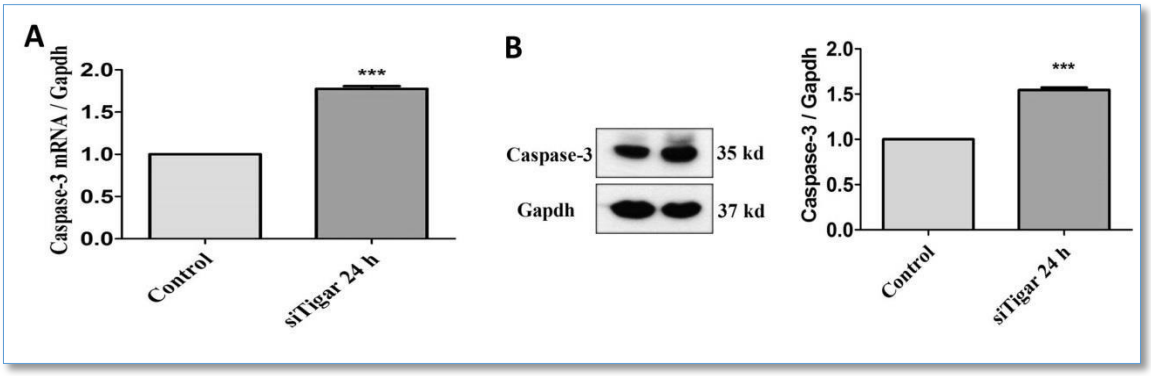

Figure 3.6. siRNA TIGAR knockdown induced apoptosis of A549 cells. Transfection of siRNAs was performed to knockdown TIGAR expression for 24 h. Expression of Caspase-3 as apoptotic marker was detected using western blotting and qRT PCR. For loading control, GAPDH, a housekeeping protein was used. Protein band intensity analysis was performed with Image J software and graphs were plotted using GraphPad Prism 5.01 software. (A) Expression of Caspase-3 mRNA levels was upregulated compared with its level in the control-A549 cell line without transfection by siTIGAR.(B) Expression of Caspase-3 protein level was upregulated compared with its level in the control-A549 cell line without transfection by siTIGAR. Data were expressed as mean ± SD with three independent experiments. (* $p< 0.05$ vs cont., ** $p<0.01$ vs cont. and *** $p<0.001$ vs cont.).

3.6. TIGAR-Specific siRNA up-Regulates Autophagy Markers

The next proteins that were studied in the A549 cell line were LC3 I, II, and Beclin-1, as autophagic markers. This experiment was done by the same procedures as mentioned earlier. Lysates were loaded at 25 µg per well for control and samples into a new gel, separated by SDS and then analyzed by western blotting; these procedures were described in section 2.9. The protein bands were labeled by using primary and secondary antibodies as mentioned in section 2.9.8. Figure 3.7 illustrates the results of the GAPDH, LC3 I, II, and Beclin-1 by western blot. They produced on the same membrane to confirm the validity of the result of LC3 I, II, and Beclin-1 expression by ensuring accuracy when loading could be determined and visualized. The molecular ladder weight marker was used. The membrane was visualized by ECL solution.

Before the presence of LC3 I, II, and Beclin-1, GAPDH protein as housekeeping protein was detected by the same procedures as mentioned earlier (see figure 3.7). The primary antibodies were used for LC3 I, II, and Beclin-1 (Anti LC3a and Beclin-1, 1:500 dilution); LC3 I, II has a predicted molecular weight of 18 and 16 kda respectively, while Beclin-1 has a predicted molecular weight of 51 kda , clearly shown by the bands in the figure. The analysis of LC3 I, II, and Beclin-1 will be discussed in the discussion section. The mRNA levels of GAPDH, LC3 I, II, and Beclin-1 were also evaluated by qRT-PCR by the same procedures as mentioned earlier.

To identify autophagic cell death mechanism in A549 cells occurred in TIGAR-silenced cells, A549 cells were transfected with siRNAs targeting TIGAR. 24 h after transfection, the cells were used in both western blots and qRT PCR assays to check the levels of autophagy markers. LC3 I, II, and Beclin-1 as cell death markers were indicated in the transfected A549 cells, which were triggered by the silencing of TIGAR expression by RNAi. Results indicated that cell growth was inhibited, with evidence of autophagic cell death after TIGAR silencing in A549 cells. Results showed that the proteins expression and mRNA levels of autophagic markers LC3 I, II, and Beclin-1 had significantly increased after silencing of TIGAR (see figure 3.7).

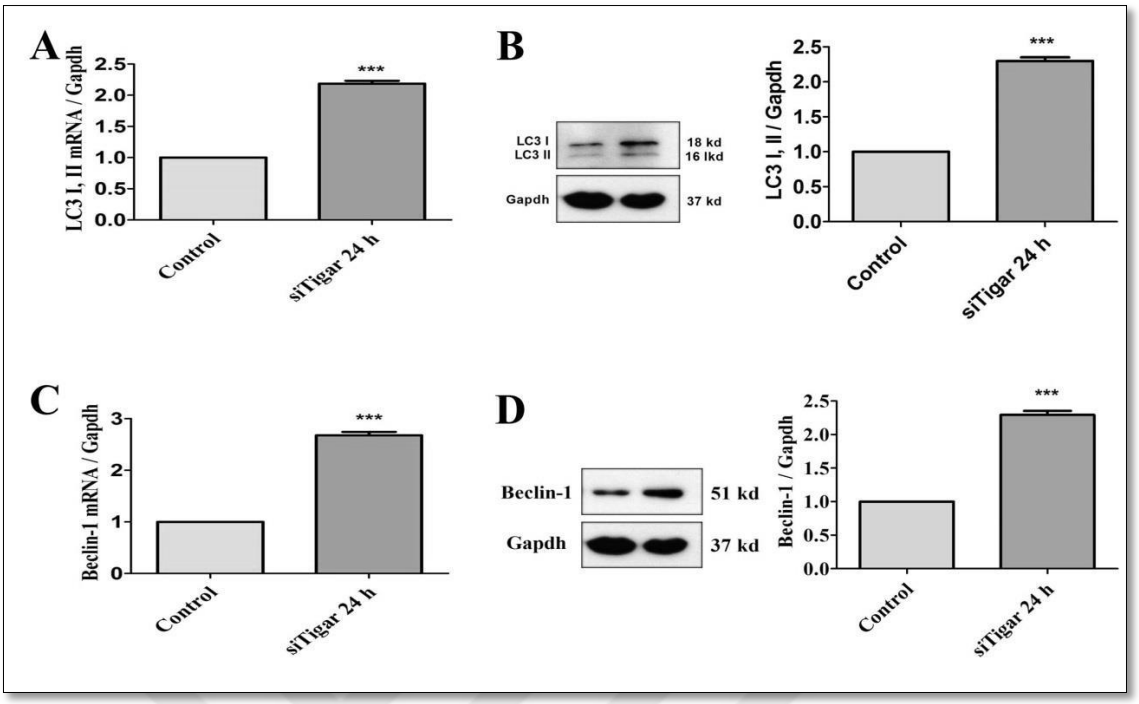

Figure 3.7. siRNA TIGAR knockdown enhances autophagy by repressing TIGAR expression. Transfection of siRNAs was performed to knockdown TIGAR expression for 24 h. The expression of LC3 I, II and Beclin-1 as autophagy markers were detected with qRT PCR and western blotting. For loading control, GAPDH, a housekeeping protein was used. Protein band intensity analysis was performed with Image J software and graphs were plotted using GraphPad Prism 5.01 software. (A) and (B) Expression of LC3 I and II mRNA and protein levels increased compared to their levels in the control-A549 cell line without transfection by siTIGAR. (C) and (D) Expression of Beclin-1 mRNA and protein levels increased compared to their levels in control-A549 cell line without transfection by siTIGAR. Data were expressed as mean ± SD with three independent experiments. (* $p< 0.05$ vs cont., ** $p<0.01$ vs cont. and *** $p<0.001$ vs cont.)

3.7. TIGAR-Specific siRNA up-Regulates Oxidative Stress Markers

The last proteins that were studied in the A549 cell line were NF-κB and HO-1, as oxidative stress markers. This experiment was done by the same procedures as mentioned earlier. Lysates were loaded at 25 µg per well for control and samples into a new gel, separated by SDS and then analyzed by western blotting; these procedures were described in section 2.9. The protein bands were labeled by using primary and secondary antibodies as mentioned in section 2.9.8. Figure 3.8 illustrates the results of the GAPDH, NF-κB and HO-1 by western blot. They produced on the same membrane to confirm the validity of the result of NF-κB and HO-1 expression by ensuring accuracy when loading could be determined and visualized. The molecular ladder weight marker was used. The membrane was visualized by ECL solution.

Before the presence of NF-κB and HO-1, GAPDH protein as housekeeping protein was detected by the same procedures as mentioned earlier (see figure 3.8). The primary antibodies were used for NF-κB and HO-1 (Anti NF-κB P65 and HO-1, 1:500 dilutions); NF-κB has a predicted molecular weight of 64, while HO-1 has a predicted molecular weight of 32 kda, clearly shown by the bands in the figure 3.8. The analysis of NF-κB and HO-1 will be discussed in the discussion section. The mRNA levels of GAPDH, NF-κB and HO-1 were also evaluated by qRT-PCR by the same procedures as mentioned earlier. To determine whether a link exists between cell death markers and oxidative stress markers, oxidative stress markers were observed. Similarly to apoptosis and autophagy markers, expression levels of both NF-κB and HO-1 increased in their proteins and mRNA levels compared with control cells (see figure 3.8).

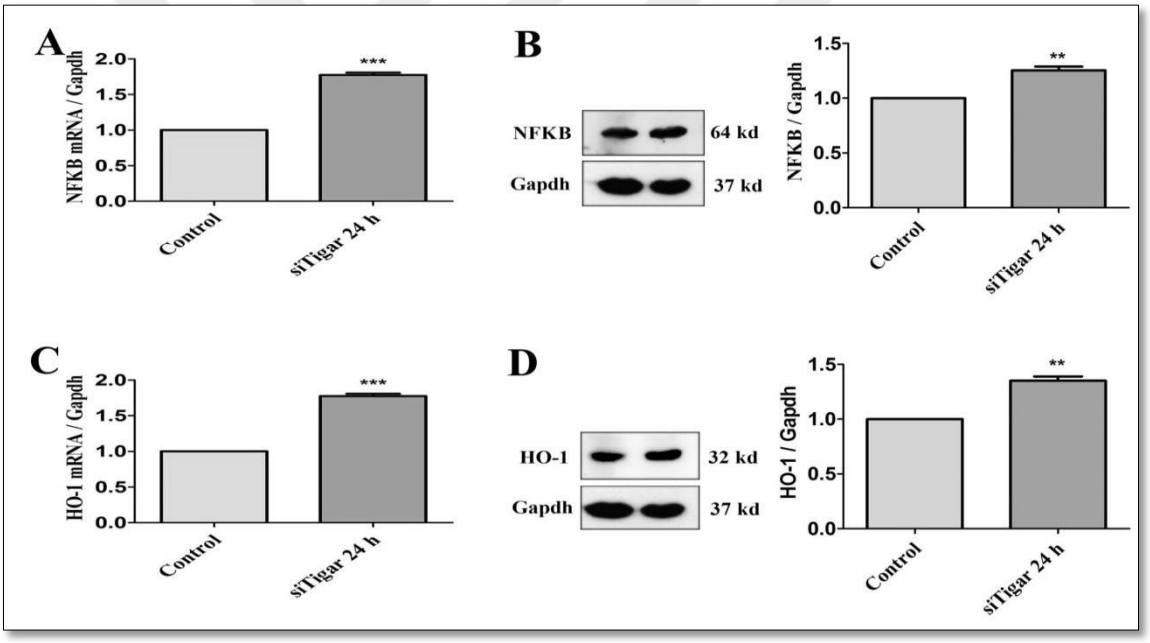

Figure 3.8. siRNA TIGAR knockdown enhances oxidative stress markers by repressing TIGAR expression. Transfection of siRNAs was performed to knockdown TIGAR expression for 24 h. The expression of NF-κB and HO-1 as oxidative stress markers were detected with qRT PCR and western blotting. For loading control, GAPDH, a housekeeping protein was used. Protein band intensity analysis was performed with Image J software and graphs were plotted using GraphPad Prism 5.01 software. (A) and (B) Expression of NF-κB mRNA and protein levels increased compared to their levels in the control-A549 cell line without transfection by siTIGAR. (C) and (D) Expression of HO-1 mRNA and protein levels increased compared to their levels in control-A549 cell line without transfection by siTIGAR. Data were expressed as mean ± SD with three independent experiments. (* $p< 0.05$ vs cont., ** $p<0.01$ vs cont. and *** $p<0.001$ vs cont.)

4. DISCUSSION

Lung cancer is the most malignant type of cancer worldwide and is responsible for high death rates (Yagi et al 2017). NSCLC accounts for nearly 85% of lung cancer cases (Molina et al 2008). Recently, the survival and prognosis rate of NSCLC patients has improved significantly as a result of effective and advanced treatment strategies; however, metastasis of this cancer still poses a major challenge in clinical settings (Fandy et al 2014). TIGAR proteins control glucose metabolism flux from glycolysis into the PPP-oxidative branch, generating NADPH, GSH, and ribose-5-phosphate, neutralizing intracellular ROS levels, and inducing DNA repair (Kumar et al 2015). TIGAR can control Fru-2, 6-P2 levels during glucose metabolism in cells, and also helps to maintain NADPH levels to recycle GSH, a key intracellular antioxidant. Therefore, silencing of TIGAR expression leads to increased ROS levels, which correlate with greater resistance to cell death. This occurs by enhancing the PPP, which directly contributes to DNA repair by generating ribose-5-phosphate and NADPH, two key precursors of DNA repair and synthesis (Bensaad et al 2009; Bensaad et al 2006; Cheung et al 2016; Lee et al 2014; Pena-Rico et al 2011).

The aim of the project was to use a siRNA TIGAR in vitro model to study the viability of the cells and the expression of key program cell death proteins in tumor-derived cell line A549, which would allow correlations to be made between protein expression levels and degree of viability. In particular, some of the parameters examined are common that are known to be differentially regulated during cellular changes associated with siRNA transfection such the inverse correlation between ROS and NADPH levels. Specifically, in order to investigate expression of apoptosis, autophagy and oxidative stress proteins in the human A549; cell viability, clonogenic, DCFDA, NADPH, western blot, and qRT PCR assays were performed as detailed in the methodology and results section

Our results indicate that the siRNA TIGAR gene is capable of inhibiting transcription of TIGAR RNA, causing upregulation of oxidative stress markers and inducing cell death in the A549 cell line. Additionally, we investigated whether the specific silencing of TIGAR by siRNA could provide a new strategy to enhance A549 cells to trigger programmed cell death via oxidative stress markers. There is a fact that might be better for more efficiency our data, both positive and negative control had to be used during transfection of TIGAR. This new strategy has the potential to be a molecularly targeted new way in gene silencing in NSCLC.

Previous studies have reported that siRNA TIGAR down-regulated TIGAR expression in glioblastoma cells, hepatocellular carcinoma, and prostate cancer (Huang et al 2017; Tai et al 2016; Wanka et al 2012; Xie et al 2014; Yu et al 2015a). Therefore, this study is a new attempt to evaluate the siTIGAR down-regulate in a lung cancer cells. To examine how siRNA TIGAR could affect cell growth and cell survival, we designed several experiments and observed their results. For this reason, A549 cell growth was studied 24 h post-transfection by cell viability assay, WST-1 kit. Cells transfected with TIGAR-siRNA showed a decrease of growth significantly less than the control cells. Consequently, colony formation was markedly lower than in the control condition (see figure 3.4).

It has been indicated that TIGAR allows cancer cells to survive by repairing gene damage after exposure to moderate levels of stress. Normally, ROS is released in low concentrations during cellular metabolism, and can be compensated for by TIGAR and other cellular antioxidant mechanisms (Pena-Rico et al 2011). The primary function of ROS participates in most cell responses, including DNA damage and cell death. Based on ROS function, inhibition and induction of intracellular ROS have been related with cancer therapy. Our results also indicated that ROS levels were slightly increased in A549 cells after TIGAR knockdown (Figure 3.5.A). TIGAR is able to maintain NADPH levels to regenerate GSH by controlling glucose metabolism; GSH is a key intracellular antioxidant. Loss of TIGAR expression leads to inhibition of the PPP and increased ROS levels (Okar et al 2001; Zhang et al 2017). Additionally to ROS level, our results also indicated that NADPH levels decreased slightly in A549 cells after TIGAR knockdown (Figure 3.5.B).

A number of studies of cancer cells have shown that TIGAR silencing is related to decreased levels of NADPH (Lui et al 2010; Lui et al 2011; Yin et al 2012) and lower levels of reduced GSH (Wong et al 2015; Ye et al 2013; Yin et al 2012), and is consequently followed by an increase in ROS (Qian et al 2016). Pen˜a-Rico and colleagues showed that TIGAR knockdown resulted in radio-sensitization of glioma cells with increased levels of Fru-2, 6-BP, lactate, and ROS, and reduced GSH levels (Pena-Rico et al 2011). Our data have shown quite same results like these studies regarding to the ROS and NADPH levels after silencing TIGAR protein.

The PPP-also known as the phosphor-gluconate pathway due to its role in supplying cancer cells with ribo-nucleotides and NADPH for intracellular anabolic processes-plays a pivotal role in apoptosis, tumor proliferation, resistance to immune-radiation and chemotherapy, angiogenesis (Patra and Hay 2014). High levels of PPP flux are known to result in more proliferative, invasive, and drug-resistant phenotypes in cancer cells (Riganti et al 2012) and may be critical for cancer treatment, if the PPP is inhibited. According to previous studies, programmed cell death I and II may also occur when TIGAR-silencing is combined with certain drugs, including adriamycin, rapamycin, epirubicin, cisplatin or an external factor such as hypoxia or radiotherapy (Huang et al 2017; Pena-Rico et al 2011; Wanka et al 2012; Xie et al 2014; Yu et al 2015b). To determine whether the decrease in cell numbers following TIGAR knockdown occurred due to cell death, we examined several mechanisms. First, we analyzed protein expression and mRNA levels of Caspase-3, an apoptotic marker that significantly increased after silencing of TIGAR 24 h post-transfection (Figure 3.6). The studies indicate that TIGAR can prevent apoptosis and autophagy by reducing ROS levels. Furthermore, the data showed that TIGAR can govern ROS accumulation and inhibit apoptosis. A previous study stated that both types of programmed cell death-autophagy and apoptosis-could occur in mammalian cells, and the induction of autophagy has been shown to enhance the apoptotic response (Zhao et al 2017).

We also examined type II programmed cell death, autophagy markers, because in response to anticancer therapies, different types of cancer cells undergo autophagy though whether autophagy in cancer protects or kills cells remains a subject of debate (Zhuang et al 2009). Furthermore results in our study, it is the upregulation of protein and

mRNA levels occurred in both autophagy markers, LC3 I, II, and in Beclin-1 (see figure 3.7). The researchers in their studies indicated that autophagy and apoptosis play dual roles in cell death (Ye et al 2013), demonstrating that differentiation malignancy of NSCLC is closely correlated with TIGAR expression. By inducing the PPP, TIGAR can limit fructose-2, 6-bisphosphatase levels. Moreover, recent studies have also illustrated TIGAR's relationship to autophagy and apoptosis, showing that TIGAR's silencing ability is strongly related to upregulation of ROS, resulting in higher intracellular NADPH levels (Xie et al 2014).

NF-κB incorporates a central importance in immunity and inflammation, additionally plays necessary roles in different processes, such as cell growth, survival and development, and proliferation, and features a role in several pathological conditions (Morgan and Liu 2011). While, in another study recommended raised ROS levels and reduced NF-κB activity after knockdown of termed thioredoxin-like 2 (TXNL2) in human carcinoma cell lines (Qu et al 2011). These are telling us there is interference between reactive oxygen species expression and NF-κB signaling. It was necessary for the purposes of this study to correlate the oxidative stress markers to siRNA TIGAR. So, to understand the relationship of oxidative stress markers to cell death types such as autophagy and apoptosis, we indicated that the expression of NF-κB was up-regulated 24 h post siTIGAR transfection (see figure 3.8 A and B), when the effect of siTIGAR of there expression were measured by western blotting and qRT PCR analysis.

The inducible variety of Heme Oxygenase-1 (HO-1) could be a major endoplasmic reticulum (ER) associated heme protein and identified to plays necessary roles in protection against chemical and oxidative stress by degrading free heme discharged from degradation of heme proteins (Bansal et al 2014). Studies recommend the contribution of chemical stress, oxidative stress and ROS inducement the expression of HO-1 (Bindu et al 2011). And it is raised to stop DNA harm caused by the ROS, HO-1 down regulation results in the rise of DNA damage and ROS in cells (Lin et al 2013). Additionally to checking NF-κB, we indicated also the expression of HO-1 that was up-regulated 24 h post siTIGAR transfection (see figure 3.8 C and D), when the effect of siTIGAR of there expression were measured by western blotting and qRT PCR analysis.

Our findings show that TIGAR has a role in programmed cell death apoptosis and autophagy. As far as we are aware of, this study provides the first evidence that knockdown of TIGAR expression provides the induction of markers of both apoptosis and autophagy levels in A549 cells via oxidative stress markers. These findings provide the possibility that TIGAR may act as an important role in protecting A549 cells from dying through apoptosis and autophagy. In addition, our data show that ROS levels may are likely to play a role in siTIGAR-induced apoptosis by expression of Caspase-3 (Figure 3.6), while expression of LC3 I and II and Beclin-1 are accountable for cell death in A549 cells as autophagy markers (Figure 3.7). However, increased ROS levels also increased levels of the oxidative stress markers NF-κB and HO-1 (Figure 3.8), which may be responsible for induction of both autophagy and apoptosis.

Furthermore, this study would allow better understanding of the process of silencing protein by siRNA and checking some more parameters to support the results. Also, it is necessary to use siRNA transfection technique in normal cell line and using animal model as well rather than cell culture model. Further experiments like (Flow cytometry, Immunofluorescence, Mitochondrial membrane potential, Comet)could be designed to test the hypotheses of this project in a more advanced manner to further understanding on the impact role of siTIGAR on the Caspase-3, Beclin-1, LC3 I, II, NF-κB and HO-1 express and correlation with program cell death.

5. CONCLUSION

This study has successfully investigated the effect of down regulation of TIGAR in A549, a representative cell line for NSCLC. For this purpose, we evaluated cell viability, colony forming activities, and the level of ROS, NADPH. Also, qRT PCR and western blot techniques were used to measure the changes in the levels of the molecule mentioned above. The success of the experiments allowed us to transfect the cell line and analyzed their behavior in relation to TIGAR molecule in malignant cells. As expected, the results of the experiments demonstrated that TIGAR loss in a cell may lead to apoptosis and autophagy by increasing ROS.

Targeting TIGAR with siRNA caused specific and efficient inhibition of endogenous TIGAR expression in A549 lung cancer cells. TIGAR silencing inhibits cell viability and colony formation and induces the implication of intracellular ROS and then reducing NADPH levels. These data suggest that TIGAR-regulated ROS induce cell death and it may be used as a potential strategy in cancer therapy, opening a new window in gene silencing therapy in lung cancer cells.

REFERENCES

Aita VM, Liang XH, Murty VV, Pincus DL, Yu W, Cayanis E, Kalachikov S, Gilliam TC, Levine B (1999) Cloning and genomic organization of beclin 1, a candidate tumor suppressor gene on chromosome 17q21. Genomics 59(1): 59-65

Alberts B. 2002. Molecular biology of the cell. New York: Garland Science

Ambegaokar SS, Kolson DL (2014) Heme oxygenase-1 dysregulation in the brain: implications for HIV-associated neurocognitive disorders. Curr HIV Res 12(3): 174-188

Arico S, Petiot A, Bauvy C, Dubbelhuis PF, Meijer AJ, Codogno P, Ogier-Denis E (2001) The tumor suppressor PTEN positively regulates macroautophagy by inhibiting the phosphatidylinositol 3-kinase/protein kinase B pathway. The Journal of biological chemistry 276(38): 35243-35246

Axe EL, Walker SA, Manifava M, Chandra P, Roderick HL, Habermann A, Griffiths G, Ktistakis NT (2008) Autophagosome formation from membrane compartments enriched in phosphatidylinositol 3-phosphate and dynamically connected to the endoplasmic reticulum. The Journal of cell biology 182(4): 685-701

Bansal S, Biswas G, Avadhani NG (2014) Mitochondria-targeted heme oxygenase-1 induces oxidative stress and mitochondrial dysfunction in macrophages, kidney fibroblasts and in chronic alcohol hepatotoxicity. Redox biology 2: 273-283

Bensaad K, Cheung EC, Vousden KH (2009) Modulation of intracellular ROS levels by TIGAR controls autophagy. The EMBO journal 28(19): 3015-3026

Bensaad K, Tsuruta A, Selak MA, Vidal MN, Nakano K, Bartrons R, Gottlieb E, Vousden KH (2006) TIGAR, a p53-inducible regulator of glycolysis and apoptosis. Cell 126(1): 107-120

Bialik S, Kimchi A (2010) Lethal weapons: DAP-kinase, autophagy and cell death: DAP-kinase regulates autophagy. Current opinion in cell biology 22(2): 199-205

Bialik S, Zalckvar E, Ber Y, Rubinstein AD, Kimchi A (2010) Systems biology analysis of programmed cell death. Trends in biochemical sciences 35(10): 556-564

Bindu S, Pal C, Dey S, Goyal M, Alam A, Iqbal MS, Dutta S, Sarkar S, Kumar R, Maity P and others (2011) Translocation of heme oxygenase-1 to mitochondria is a novel cytoprotective mechanism against non-steroidal anti-inflammatory drug-induced mitochondrial oxidative stress, apoptosis, and gastric mucosal injury. The Journal of biological chemistry 286(45): 39387-39402

Birgisdottir ÅB, Lamark T, Johansen T (2013) The LIR motif – crucial for selective autophagy. Journal of Cell Science 126(15): 3237-3247

Chang WT, Cheng HL, Hsieh BS, Chiu CC, Lee KT, Chang KL (2014) Progesterone increases apoptosis and inversely decreases autophagy in human hepatoma HA22T/VGH cells treated with epirubicin. ScientificWorldJournal 2014: 567148

Chen N, Karantza V (2011) Autophagy as a therapeutic target in cancer. Cancer biology & therapy 11(2): 157-168

Chen S, Li P, Li J, Wang Y, Du Y, Chen X, Zang W, Wang H, Chu H, Zhao G and others (2015) MiR-144 inhibits proliferation and induces apoptosis and autophagy in lung cancer cells by targeting TIGAR. Cellular physiology and biochemistry : international journal of experimental cellular physiology, biochemistry, and pharmacology 35(3): 997-1007

Chen S, Rehman SK, Zhang W, Wen A, Yao L, Zhang J (2010) Autophagy is a therapeutic target in anticancer drug resistance. Biochimica et biophysica acta 1806(2): 220-229

Cheung EC, Lee P, Ceteci F, Nixon C, Blyth K, Sansom OJ, Vousden KH (2016) Opposing effects of TIGAR- and RAC1-derived ROS on Wnt-driven proliferation in the mouse intestine. Genes & development 30(1): 52-63

Cheung EC, Ludwig RL, Vousden KH (2012) Mitochondrial localization of TIGAR under hypoxia stimulates HK2 and lowers ROS and cell death. Proceedings of the National Academy of Sciences of the United States of America 109(50): 20491-20496

Choi KS (2012) Autophagy and cancer. Experimental & molecular medicine 44(2): 109-120

Degenhardt K, Mathew R, Beaudoin B, Bray K, Anderson D, Chen G, Mukherjee C, Shi Y, Gelinas C, Fan Y and others (2006) Autophagy promotes tumor cell survival and restricts necrosis, inflammation, and tumorigenesis. Cancer cell 10(1): 51-64

Deter RL, De Duve C (1967) Influence of glucagon, an inducer of cellular autophagy, on some physical properties of rat liver lysosomes. The Journal of cell biology 33(2): 437-449

Diaz-Troya S, Perez-Perez ME, Florencio FJ, Crespo JL (2008) The role of TOR in autophagy regulation from yeast to plants and mammals. Autophagy 4(7): 851-865

Edinger AL, Thompson CB (2004) Death by design: apoptosis, necrosis and autophagy. Current Opinion in Cell Biology 16(6): 663-669

Egan DF, Shackelford DB, Mihaylova MM, Gelino S, Kohnz RA, Mair W, Vasquez DS, Joshi A, Gwinn DM, Taylor R and others (2011) Phosphorylation of ULK1 (hATG1) by AMP-activated protein kinase connects energy sensing to mitophagy. Science (New York, NY) 331(6016): 456-461

Eisenberg-Lerner A, Bialik S, Simon HU, Kimchi A (2009) Life and death partners: apoptosis, autophagy and the cross-talk between them. Cell death and differentiation 16(7): 966-975

El-Khattouti A, Selimovic D, Haikel Y, Hassan M (2013) Crosstalk between apoptosis and autophagy: molecular mechanisms and therapeutic strategies in cancer. J Cell Death 6: 37-55

Elmore S (2007) Apoptosis: a review of programmed cell death. Toxicologic pathology 35(4): 495-516

Ernst O, Zor T (2010) Linearization of the Bradford Protein Assay. Journal of Visualized Experiments : JoVE(38): 1918

Fandy TE, Jiemjit A, Thakar M, Rhoden P, Suarez L, Gore SD (2014) Decitabine induces delayed reactive oxygen species (ROS) accumulation in leukemia cells and induces the expression of ROS generating enzymes. Clinical cancer research : an official journal of the American Association for Cancer Research 20(5): 1249-1258

Filomeni G, De Zio D, Cecconi F (2014) Oxidative stress and autophagy: the clash between damage and metabolic needs. Cell Death And Differentiation 22: 377

Futreal PA, Soderkvist P, Marks JR, Iglehart JD, Cochran C, Barrett JC, Wiseman RW (1992) Detection of frequent allelic loss on proximal chromosome 17q in sporadic breast carcinoma using microsatellite length polymorphisms. Cancer research 52(9): 2624-2627

Gao X, Zacharek A, Salkowski A, Grignon DJ, Sakr W, Porter AT, Honn KV (1995) Loss of heterozygosity of the BRCA1 and other loci on chromosome 17q in human prostate cancer. Cancer research 55(5): 1002-1005

Glick D, Barth S, Macleod KF (2010) Autophagy: cellular and molecular mechanisms. The Journal of pathology 221(1): 3-12

Gozuacik D, Kimchi A (2004) Autophagy as a cell death and tumor suppressor mechanism. Oncogene 23(16): 2891-2906

Hanahan D, Weinberg RA (2011) Hallmarks of cancer: the next generation. Cell 144(5):646-674

He C, Klionsky DJ (2009) Regulation mechanisms and signaling pathways of autophagy. Annual review of genetics 43: 67-93

Huang S, Yang Z, Ma Y, Yang Y, Wang S (2017) miR-101 Enhances Cisplatin-Induced DNA Damage Through Decreasing Nicotinamide Adenine Dinucleotide Phosphate Levels by Directly Repressing Tp53-Induced Glycolysis and Apoptosis Regulator Expression in Prostate Cancer Cells. DNA and cell biology 36(4): 303-310

Huett A, Goel G, Xavier RJ (2010) A systems biology viewpoint on autophagy in health and disease. Current opinion in gastroenterology 26(4): 302-309

Islami F, Torre LA, Jemal A (2015) Global trends of lung cancer mortality and smoking prevalence. Translational lung cancer research 4(4): 327-338

Jackson SP, Bartek J (2009) The DNA-damage response in human biology and disease. Nature 461: 1071

Janku F, McConkey DJ, Hong DS, Kurzrock R (2011) Autophagy as a target for anticancer therapy. Nature reviews Clinical oncology 8(9): 528-539

Jen KY, Cheung VG (2005) Identification of novel p53 target genes in ionizing radiation response. Cancer research 65(17): 7666-7673

Jiang L, DeBerardinis RJ (2012) When more is less. Nature 489: 511

John TS (2005) With Every Breath: A Lung Cancer Guidebook. Vancouver: Alliance for Lung Cancer Advocacy Support & Education (ALCASE)

Kalemkerian GP, Donington JS, Gore EM, Ramalingam SS (2016) Handbook of lung cancer and other thoracic malignancies. New York: Demos Medical. 415 p

Kanzawa T, Zhang L, Xiao L, Germano IM, Kondo Y, Kondo S (2005) Arsenic trioxide induces autophagic cell death in malignant glioma cells by upregulation of mitochondrial cell death protein BNIP3. Oncogene 24(6): 980-991

Kannan K, Jain SK (2000) Oxidative stress and apoptosis. Pathophysiology 7(3): 153-163

Kanzawa T, Zhang L, Xiao L, Germano IM, Kondo Y, Kondo S (2005) Arsenic trioxide induces autophagic cell death in malignant glioma cells by upregulation of mitochondrial cell death protein BNIP3. Oncogene 24(6): 980-991

Kara Rogers Senior Editor BS (2010) The Respiratory System: Britannica Educational Pub

Karantza-Wadsworth V, Patel S, Kravchuk O, Chen G, Mathew R, Jin S, White E (2007) Autophagy mitigates metabolic stress and genome damage in mammary tumorigenesis. Genes & development 21(13): 1621-1635

Kerr JF, Wyllie AH, Currie AR (1972) Apoptosis: a basic biological phenomenon with wide-ranging implications in tissue kinetics. British journal of cancer 26(4): 239-257

Kirisako T, Baba M, Ishihara N, Miyazawa K, Ohsumi M, Yoshimori T, Noda T, Ohsumi Y (1999) Formation process of autophagosome is traced with Apg8/Aut7p in yeast. The Journal of cell biology 147(2): 435-446

Klionsky DJ (2005) The molecular machinery of autophagy: unanswered questions. Journal of cell science 118(Pt 1): 7-18

Kondo Y, Kanzawa T, Sawaya R, Kondo S (2005) The role of autophagy in cancer development and response to therapy. Nature reviews Cancer 5(9): 726-734

Kumar B, Iqbal MA, Singh RK, Bamezai RN (2015) Resveratrol inhibits TIGAR to promote ROS induced apoptosis and autophagy. Biochimie 118: 26-35

Kundu M, Thompson CB (2008) Autophagy: basic principles and relevance to disease. Annual review of pathology 3: 427-455

Lawrence T (2009) The nuclear factor NF-kappaB pathway in inflammation. Cold Spring Harb Perspect Biol 1(6): a001651

Lee P, Vousden KH, Cheung EC (2014) TIGAR, TIGAR, burning bright. Cancer & metabolism 2(1): 1

Levine B, Klionsky DJ (2004) Development by self-digestion: molecular mechanisms and biological functions of autophagy. Developmental cell 6(4): 463-477

Levine B, Yuan J (2005) Autophagy in cell death: an innocent convict? The Journal of clinical investigation 115(10): 2679-2688

Li L, Tan J, Miao Y, Lei P, Zhang Q (2015) ROS and Autophagy: Interactions and Molecular Regulatory Mechanisms. Cellular and molecular neurobiology 35(5): 615-621

Li M, Sun M, Cao L, Gu JH, Ge J, Chen J, Han R, Qin YY, Zhou ZP, Ding Y and others (2014) A TIGAR-regulated metabolic pathway is critical for protection of brain ischemia. The Journal of neuroscience : the official journal of the Society for Neuroscience 34(22): 7458-7471

Li WW, Li J, Bao JK (2012) Microautophagy: lesser-known self-eating. Cellular and molecular life sciences : CMLS 69(7): 1125-1136

Li ZY, Yang Y, Ming M, Liu B (2011) Mitochondrial ROS generation for regulation of autophagic pathways in cancer. Biochemical and biophysical research communications 414(1): 5-8

Liang C, Feng P, Ku B, Dotan I, Canaani D, Oh BH, Jung JU (2006) Autophagic and tumour suppressor activity of a novel Beclin1-binding protein UVRAG. Nature cell biology 8(7): 688-699

Liang J, Shao SH, Xu ZX, Hennessy B, Ding Z, Larrea M, Kondo S, Dumont DJ, Gutterman JU, Walker CL and others (2007) The energy sensing LKB1-AMPK pathway regulates p27(kip1) phosphorylation mediating the decision to enter autophagy or apoptosis. Nature cell biology 9(2): 218-224

Lin PH, Lan WM, Chau LY (2013) TRC8 suppresses tumorigenesis through targeting heme oxygenase-1 for ubiquitination and degradation. Oncogene 32(18): 2325-2334

Liu B, Bao JK, Yang JM, Cheng Y (2013) Targeting autophagic pathways for cancer drug discovery. Chinese journal of cancer 32(3): 113-120

Liu JJ, Lin M, Yu JY, Liu B, Bao JK (2011) Targeting apoptotic and autophagic pathways for cancer therapeutics. Cancer letters 300(2): 105-114

Livak KJ, Schmittgen TD (2001) Analysis of relative gene expression data using real-time quantitative PCR and the 2(-Delta Delta C(T)) Method. Methods (San Diego, Calif) 25(4): 402-408

Lowe SW, Lin AW (2000) Apoptosis in cancer. Carcinogenesis 21(3): 485-495

Lui VW, Lau CP, Cheung CS, Ho K, Ng MH, Cheng SH, Hong B, Tsao SW, Tsang CM, Lei KI and others (2010) An RNA-directed nucleoside anti-metabolite, 1-(3-C-ethynyl-beta-d-ribo-pentofuranosyl)cytosine (ECyd), elicits antitumor effect via TP53-induced Glycolysis and Apoptosis Regulator (TIGAR) downregulation. Biochemical pharmacology 79(12): 1772-1780

Lui VW, Wong EY, Ho K, Ng PK, Lau CP, Tsui SK, Tsang CM, Tsao SW, Cheng SH, Ng MH and others (2011) Inhibition of c-Met downregulates TIGAR expression and reduces NADPH production leading to cell death. Oncogene 30(9): 1127-1134

Lum JJ, Bauer DE, Kong M, Harris MH, Li C, Lindsten T, Thompson CB (2005) Growth factor regulation of autophagy and cell survival in the absence of apoptosis. Cell 120(2): 237-248

Luo Z, Zang M, Guo W (2010) AMPK as a metabolic tumor suppressor: control of metabolism and cell growth. Future oncology (London, England) 6(3): 457-470

Luthi AU, Martin SJ (2007) The CASBAH: a searchable database of caspase substrates. Cell death and differentiation 14(4): 641-650

Mahmood T, Yang PC (2012) Western blot: technique, theory, and trouble shooting. North American journal of medical sciences 4(9): 429-434

Maiuri MC, Criollo A, Tasdemir E, Vicencio JM, Tajeddine N, Hickman JA, Geneste O, Kroemer G (2007)a BH3-only proteins and BH3 mimetics induce autophagy by competitively disrupting the interaction between Beclin 1 and Bcl-2/Bcl-X(L). Autophagy 3(4): 374-376

Maiuri MC, Galluzzi L, Morselli E, Kepp O, Malik SA, Kroemer G (2010) Autophagy regulation by p53. Current opinion in cell biology 22(2): 181-185

Maiuri MC, Zalckvar E, Kimchi A, Kroemer G (2007)b Self-eating and self-killing: crosstalk between autophagy and apoptosis. Nature reviews Molecular cell biology 8(9): 741-752

Marino G, Salvador-Montoliu N, Fueyo A, Knecht E, Mizushima N, Lopez-Otin C (2007) Tissue-specific autophagy alterations and increased tumorigenesis in mice deficient in Atg4C/autophagin-3. The Journal of biological chemistry 282(25): 18573-18583

Mathew R, Karp CM, Beaudoin B, Vuong N, Chen G, Chen HY, Bray K, Reddy A, Bhanot G, Gelinas C and others (2009) Autophagy suppresses tumorigenesis through elimination of p62. Cell 137(6): 1062-1075

Mathew R, Kongara S, Beaudoin B, Karp CM, Bray K, Degenhardt K, Chen G, Jin S, White E (2007) Autophagy suppresses tumor progression by limiting chromosomal instability. Genes & development 21(11): 1367-1381

Mathew R, White E (2011) Autophagy, stress, and cancer metabolism: what doesn't kill you makes you stronger. Cold Spring Harbor symposia on quantitative biology 76: 389-396

Mizushima N (2007) Autophagy: process and function. Genes & development 21(22): 2861-2873

Molina JR, Yang P, Cassivi SD, Schild SE, Adjei AA (2008) Non-small cell lung cancer: epidemiology, risk factors, treatment, and survivorship. Mayo Clinic proceedings 83(5): 584-594

Morgan MJ, Liu ZG (2011) Crosstalk of reactive oxygen species and NF-kappaB signaling. Cell research 21(1): 103-115

Morselli E, Galluzzi L, Kepp O, Vicencio JM, Criollo A, Maiuri MC, Kroemer G (2009) Anti- and pro-tumor functions of autophagy. Biochimica et biophysica acta 1793(9): 1524-1532

Mothoneos J (2016) Understanding Lung Cancer: A guide for people with cancer, their families and friends. Sydney: Cancer Council Australia

Narayanan A, Amaya M, Voss K, Chung M, Benedict A, Sampey G, Kehn-Hall K, Luchini A, Liotta L, Bailey C and others (2014) Reactive oxygen species activate NFkappaB (p65) and p53 and induce apoptosis in RVFV infected liver cells. Virology 449: 270-286

Nikoletopoulou V, Markaki M, Palikaras K, Tavernarakis N (2013) Crosstalk between apoptosis, necrosis and autophagy. Biochim Biophys Acta 1833(12): 3448-3459

Nishida K, Yamaguchi O, Otsu K (2008) Crosstalk between autophagy and apoptosis in heart disease. Circulation research 103(4): 343-351

Okar DA, Manzano A, Navarro-Sabate A, Riera L, Bartrons R, Lange AJ (2001) PFK-2/FBPase-2: maker and breaker of the essential biofactor fructose-2,6-bisphosphate. Trends in biochemical sciences 26(1): 30-35

Oliver KM, Garvey JF, Ng CT, Veale DJ, Fearon U, Cummins EP, Taylor CT (2009) Hypoxia activates NF-kappaB-dependent gene expression through the canonical signaling pathway. Antioxid Redox Signal 11(9): 2057-2064

Ouyang L, Shi Z, Zhao S, Wang FT, Zhou TT, Liu B, Bao JK (2012) Programmed cell death pathways in cancer: a review of apoptosis, autophagy and programmed necrosis. Cell proliferation 45(6): 487-498

Patient T, Centre FR (2017) Understanding Lung Cancer Information for individuals with lung cancer and their families. Hamilton Ontario: Juravinski Cancer Centre

Patra KC, Hay N (2014) The pentose phosphate pathway and cancer. Trends in biochemical sciences 39(8): 347-354

Pena-Rico MA, Calvo-Vidal MN, Villalonga-Planells R, Martinez-Soler F, Gimenez-Bonafe P, Navarro-Sabate A, Tortosa A, Bartrons R, Manzano A (2011) TP53 induced glycolysis and apoptosis regulator (TIGAR) knockdown results in radiosensitization of glioma cells. Radiotherapy and oncology : journal of the European Society for Therapeutic Radiology and Oncology 101(1): 132-139

Prasad S, Gupta SC, Pandey MK, Tyagi AK, Deb L (2016) Oxidative Stress and Cancer: Advances and Challenges. Oxidative Medicine and Cellular Longevity 2016: 1

Qian S, Li J, Hong M, Zhu Y, Zhao H, Xie Y, Huang J, Lian Y, Li Y, Wang S and others (2016) TIGAR cooperated with glycolysis to inhibit the apoptosis of leukemia cells and associated with poor prognosis in patients with cytogenetically normal acute myeloid leukemia. Journal of hematology & oncology 9(1): 128

Qu X, Yu J, Bhagat G, Furuya N, Hibshoosh H, Troxel A, Rosen J, Eskelinen EL, Mizushima N, Ohsumi Y and others (2003) Promotion of tumorigenesis by heterozygous disruption of the beclin 1 autophagy gene. The Journal of clinical investigation 112(12): 1809-1820

Qu Y, Wang J, Ray PS, Guo H, Huang J, Shin-Sim M, Bukoye BA, Liu B, Lee AV, Lin X and others (2011) Thioredoxin-like 2 regulates human cancer cell growth and metastasis via redox homeostasis and NF-kappaB signaling. J Clin Invest 121(1): 212-225

Rahal A, Kumar A, Singh V, Yadav B, Tiwari R, Chakraborty S, Dhama K (2014) Oxidative Stress, Prooxidants, and Antioxidants: The Interplay. BioMed Research International 2014: 19

Reggiori F, Klionsky DJ (2005) Autophagosomes: biogenesis from scratch? Current opinion in cell biology 17(4): 415-422

Riganti C, Gazzano E, Polimeni M, Aldieri E, Ghigo D (2012) The pentose phosphate pathway: an antioxidant defense and a crossroad in tumor cell fate. Free radical biology & medicine 53(3): 421-436

Rouschop KM, Wouters BG (2009) Regulation of autophagy through multiple independent hypoxic signaling pathways. Current molecular medicine 9(4): 417-424

Sabatini DM (2006) mTOR and cancer: insights into a complex relationship. Nature reviews Cancer 6(9): 729-734

Ryter SW, Kim HP, Hoetzel A, Park JW, Nakahira K, Wang X, Choi AM (2007) Mechanisms of cell death in oxidative stress. Antioxid Redox Signal 9(1): 49-89

Sabatini DM (2006) mTOR and cancer: insights into a complex relationship. Nature reviews Cancer 6(9): 729-734

Sahoo S, Meijles DN, Pagano PJ (2016) NADPH oxidases: key modulators in aging and age-related cardiovascular diseases? Clinical science (London, England : 1979) 130(5): 317-335

Sambrook J, Fritsch EF, Maniatis T (1989) Molecular cloning: a laboratory manual. Cold Spring Harbor, NY: Cold Spring Harbor Laboratory Press. xxxviii + 1546 pp

Sánchez-Valle J, Tejero H, Ibáñez K, Portero JL, Krallinger M, Al-Shahrour F, Tabarés-Seisdedos R, Baudot A, Valencia A (2017) A molecular hypothesis to explain direct and inverse co-morbidities between Alzheimer's Disease, Glioblastoma and Lung cancer. Scientific Reports 7(1): 4474

Scherz-Shouval R, Elazar Z (2007) ROS, mitochondria and the regulation of autophagy. Trends in cell biology 17(9): 422-427

Scherz-Shouval R, Elazar Z (2011) Regulation of autophagy by ROS: physiology and pathology. Trends in biochemical sciences 36(1): 30-38

Senftleben U, Cao Y, Xiao G, Greten FR, Krahn G, Bonizzi G, Chen Y, Hu Y, Fong A, Sun SC and others (2001) Activation by IKKalpha of a second, evolutionary conserved, NF-kappa B signaling pathway. Science 293(5534): 1495-1499

Shao Y, Gao Z, Marks PA, Jiang X (2004) Apoptotic and autophagic cell death induced by histone deacetylase inhibitors. Proceedings of the National Academy of Sciences of the United States of America 101(52): 18030-18035

Shen HM, Codogno P (2011) Autophagic cell death: Loch Ness monster or endangered species? Autophagy 7(5): 457-465

Simonsen A, Tooze SA (2009) Coordination of membrane events during autophagy by multiple class III PI3-kinase complexes. The Journal of cell biology 186(6): 773-782

Siomek A (2012) NF-kappaB signaling pathway and free radical impact. Acta Biochim Pol 59(3): 323-331

Skonieczna M, Hejmo T, Poterala-Hejmo A, Cieslar-Pobuda A, Buldak RJ (2017) NADPH Oxidases: Insights into Selected Functions and Mechanisms of Action in Cancer and Stem Cells. Oxidative Medicine and Cellular Longevity 2017: 15

Su M, Mei Y, Sinha S (2013) Role of the Crosstalk between Autophagy and Apoptosis in Cancer. Journal of Oncology 2013: 14

Su Z, Yang Z, Xu Y, Chen Y, Yu Q (2015) Apoptosis, autophagy, necroptosis, and cancer metastasis. Mol Cancer 14:48

Sun Y, Peng Z-L (2008) Autophagy, Beclin 1, and Their Relation To Oncogenesis. Laboratory Medicine 39(5): 287-290

Sun Y, Peng ZL (2009) Programmed cell death and cancer. Postgraduate medical journal 85(1001): 134-140

Tai G, Gu P, Zhang H, He X, Du J, Huang J, Yu J, Cai J, Liu F (2016) TP53 induced glycolysis and apoptosis regulator knockdown radiosensitizes glioma cells through oxidative stress-induced excessive autophagy. International Journal of Clinical and Experimental Pathology 9(12): 7

Takahashi Y, Coppola D, Matsushita N, Cualing HD, Sun M, Sato Y, Liang C, Jung JU, Cheng JQ, Mule JJ and others (2007) Bif-1 interacts with Beclin 1 through UVRAG and regulates autophagy and tumorigenesis. Nature cell biology 9(10): 1142-1151

Tenhunen R, Marver HS, Schmid R (1969) Microsomal heme oxygenase. Characterization of the enzyme. The Journal of biological chemistry 244(23): 6388-6394

Turcotte S, Chan DA, Sutphin PD, Hay MP, Denny WA, Giaccia AJ (2008) A molecule targeting VHL-deficient renal cell carcinoma that induces autophagy. Cancer cell 14(1): 90-102

Vander Heiden MG (2011) Targeting cancer metabolism: a therapeutic window opens. Nature reviews Drug discovery 10(9): 671-684

Wang SY, Yu QJ, Zhang RD, Liu B (2011) Core signaling pathways of survival/death in autophagy-related cancer networks. The international journal of biochemistry & cell biology 43(9): 1263-1266

Wanka C, Steinbach JP, Rieger J (2012) Tp53-induced glycolysis and apoptosis regulator (TIGAR) protects glioma cells from starvation-induced cell death by up-regulating respiration and improving cellular redox homeostasis. The Journal of biological chemistry 287(40): 33436-33446

Wei Y, Pattingre S, Sinha S, Bassik M, Levine B (2008) JNK1-mediated phosphorylation of Bcl-2 regulates starvation-induced autophagy. Molecular cell 30(6): 678-688

White E (2012) Deconvoluting the context-dependent role for autophagy in cancer. Nature reviews Cancer 12(6): 401-410

White E (2015) The role for autophagy in cancer. The Journal of clinical investigation 125(1): 42-46

White E, DiPaola RS (2009) The Double-Edged Sword of Autophagy Modulation in Cancer. Clinical Cancer Research 15(17): 5308-5316

Won KY, Lim SJ, Kim GY, Kim YW, Han SA, Song JY, Lee DK (2012) Regulatory role of p53 in cancer metabolism via SCO2 and TIGAR in human breast cancer. Human pathology 43(2): 221-228

Wong EY, Wong SC, Chan CM, Lam EK, Ho LY, Lau CP, Au TC, Chan AK, Tsang CM, Tsao SW and others (2015) TP53-induced glycolysis and apoptosis regulator promotes proliferation and invasiveness of nasopharyngeal carcinoma cells. Oncology letters 9(2): 569-574

Xie JM, Li B, Yu HP, Gao QG, Li W, Wu HR, Qin ZH (2014) TIGAR has a dual role in cancer cell survival through regulating apoptosis and autophagy. Cancer research 74(18):5127-5138.

Xie Z, Klionsky DJ. 2007. Autophagosome formation: core machinery and adaptations. Nature cell biology 9(10): 1102-1109

Yagi S, Koh Y, Akamatsu H, Kanai K, Hayata A, Tokudome N, Akamatsu K, Endo K, Nakamura S, Higuchi M and others (2017) Development of an automated size-based filtration system for isolation of circulating tumor cells in lung cancer patients. PloS one 12(6): e0179744

Yang ZJ, Chee CE, Huang S, Sinicrope FA (2011) The role of autophagy in cancer: therapeutic implications. Molecular cancer therapeutics 10(9): 1533-1541

Ye L, Zhao X, Lu J, Qian G, Zheng JC, Ge S (2013) Knockdown of TIGAR by RNA interference induces apoptosis and autophagy in HepG2 hepatocellular carcinoma cells. Biochemical and biophysical research communications 437(2): 300-306

Yin L, Kosugi M, Kufe D (2012) Inhibition of the MUC1-C oncoprotein induces multiple myeloma cell death by down-regulating TIGAR expression and depleting NADPH. Blood 119(3): 810-816

Yin L, Kufe T, Avigan D, Kufe D (2014) Targeting MUC1-C is synergistic with bortezomib in downregulating TIGAR and inducing ROS-mediated myeloma cell death. Blood 123(19): 2997-3006

Yu H-P, Xie J-M, Li B, Sun Y-H, Gao Q-G, Ding Z-H, Wu H-R, Qin Z-H (2015)a TIGAR regulates DNA damage and repair through pentosephosphate pathway and Cdk5-ATM pathway. Scientific Reports 5: 9853

Yu HP, Xie JM, Li B, Sun YH, Gao QG, Ding ZH, Wu HR, Qin ZH (2015)b TIGAR regulates DNA damage and repair through pentosephosphate pathway and Cdk5-ATM pathway. Scientific reports 5: 9853

Yue Z, Jin S, Yang C, Levine AJ, Heintz N (2003) Beclin 1, an autophagy gene essential for early embryonic development, is a haploinsufficient tumor suppressor. Proceedings of the National Academy of Sciences of the United States of America 100(25): 15077-15082

Zhang Y, Chen F, Tai G, Wang J, Shang J, Zhang B, Wang P, Huang B, Du J, Yu J and others (2017) TIGAR knockdown radiosensitizes TrxR1-overexpressing glioma in vitro and in vivo via inhibiting Trx1 nuclear transport. Scientific reports 7: 42928

Zhao D, Han W, Liu X, Cui D, Chen Y (2017) Deguelin inhibits epithelial-to-mesenchymal transition and metastasis of human non-small cell lung cancer cells by regulating NIMA-related kinase 2. Thoracic cancer 8(4): 320-327

Zhou X, Ikenoue T, Chen X, Li L, Inoki K, Guan KL (2009) Rheb controls misfolded protein metabolism by inhibiting aggresome formation and autophagy. Proceedings of the National Academy of Sciences of the United States of America 106(22): 8923-8928

Zhuang W, Qin Z, Liang Z (2009) The role of autophagy in sensitizing malignant glioma cells to radiation therapy. Acta biochimica et biophysica Sinica 41(5): 341-351

CURRICULUM VITAE

Osama Hamid SHAREEF was born from Al-Sulaymaniyah/Iraq in 1985. After completing his primary and secondary education in Said-Sadiq, he graduated in 2009 from Koya University-Iraq, college of science, department of biology. Between 2010 and 2011, he completed pre-sessional English program 3 terms / full time in the international centre-University of Huddersfield / UK. Afterward, he completed his master in science with distinction ‘‘First Class’’ in Analytical Bioscience – Department of chemical and biological science in University of Huddersfield / UK between 2011 and 2012. In 2013, he was appointed as assistant lecturer in Halabja Technical Institute - Sulaimani Polytechnic University. In Feb-2015, he started his PhD education at Bingöl University-institute of science in the department of biology and now it’s a time for his PhD graduation (Jan-2019). He married and has two children with named ‘Maily and Ahmad’.